Eur. Phys. J. C 54, 89–106 (2008)
DOI 10.1140/epjc/s10052-007-0496-z

THE EUROPEAN PHYSICAL JOURNAL C

Regular Article – Theoretical Physics

Radiative decays with light scalar mesons and singlet–octet mixing in ChPT

S.A. Ivashyn[a], A.Y. Korchin[b]

Institute for Theoretical Physics, NSC Kharkov Institute of Physics and Technology, 1, Akademicheskaya St., Kharkiv 61108, Ukraine

Received: 2 August 2007 / Revised version: 13 November 2007 /
Published online: 10 January 2008 –

Abstract. We study different types of radiative decays involving $f_0(980)$ and $a_0(980)$ mesons within a unified ChPT-based approach at one-loop level. Light scalar resonances, which are seen in the $\pi\pi$, $\pi\eta$ and $K\bar{K}$ channels of the $\phi(1020)$ radiative decays and in the J/ψ decays are responsible for key questions of low-energy dynamics in the strong interaction sector, and the decays $\phi(1020) \to \gamma a_0(980)$, $\phi(1020) \to \gamma f_0(980)$, $a_0(980) \to \gamma\gamma$ and $f_0(980) \to \gamma\gamma$ are of interest for current experimental programs in Jülich, Frascati and Novosibirsk. From the theoretical point of view it is important to verify whether light scalar mesons are members of some flavor octet or nonet. We find a value for the mixing angle dictated by consistency with experiment and the coupling structures of the ChPT Lagrangian. The decay widths $f_0(980)/a_0(980) \to \gamma\rho(770)/\omega(782)$, which have not been experimentally studied yet, are predicted. We also obtain several relations between the widths, which hold independently of the coupling constants and which represent a fingerprint of the model.

PACS. 11.30.Hv; 12.39.Fe; 13.30.Eg; 14.40.-n

1 Introduction

The scalar mesons $a_0(980)$ $(I^G(J^{PC}) = 1^-(0^{++}))$ and $f_0(980)$ $(I^G(J^{PC}) = 0^+(0^{++}))$ have been discussed for more than 30 years. The shapes of the $\pi\pi$ (and $\pi\eta$) invariant mass distributions in different reactions point to these resonances. A promising source of information on the scalar mesons are the radiative decays in which scalar mesons are involved. Much experimental attention has been paid so far to the processes $\phi(1020) \to \gamma a_0$ [1] and $\phi(1020) \to \gamma f_0$ [2–4] due to the motivation put forward in [5]. A recent example of a model describing such features in the rare $\phi \to \gamma S \to \gamma\pi\eta$ $(\gamma\pi\pi)$ decays is the chiral approach with derivative couplings [6]. Among other well-known processes involving the scalar resonances one can think of $J/\psi \to \phi f_0(980) \to \phi\pi\pi$ (and $\to \phi K\bar{K}$) studied at BES [7] and nucleon–nucleon (as well as deuteron–deuteron) reactions with various hadronic final states. The transitions $a_0 \to \gamma\gamma$ and $f_0 \to \gamma\gamma$ are relevant for numerous reactions, where two-photon interactions produce miscellaneous hadronic final states. Many experiments involving $\gamma\gamma \to \pi\pi$ (or $\pi\eta$) have been carried out or are being planned.

The properties of the scalar mesons are not well understood. Nevertheless, the dominant decay channels are known to be $\pi\pi$ for the f_0 meson and $\pi\eta$ for a_0, and the total widths are in between 40 and 100 MeV. The decays to strange mesons $a_0 \to K\bar{K}$ and $f_0 \to K\bar{K}$ are dynamically allowed, though the masses of $a_0(980)$ and $f_0(980)$ may lie slightly below the $K\bar{K}$ threshold. The masses of $a_0(980)$ and $f_0(980)$ are approximately equal.

The internal structure of the light scalar mesons is also not clear. Recent advances in understanding of their structure are presented in the review of [8]. Most studies show that the light scalar meson structure cannot be explained in simple quark models. This is probably related to the special role played by these mesons in the low-energy dynamics of the strong interaction [9, 10]. Namely, scalar fields can be viewed as the Higgs sector of the strong interaction, i.e. their non-zero vacuum expectation value leads to chiral symmetry breaking and directly reflect the structure of the quark condensate in quantum chromodynamics (QCD). Some authors emphasize the proximity of the $K\bar{K}$ threshold to the a_0 and f_0 masses, which favors the presence of the molecular $K\bar{K}$ component [11] (for recent calculations implementing the molecular $K\bar{K}$ model, see [12–14].)

Another approach to light scalar meson features is unitarized ChPT [15]. In this approach the inverse amplitude method [16] was employed to describe elastic $\pi\pi$, $\pi\eta$, $K\eta$ and $K\bar{K}$ scattering data. The radiative decays in question were evaluated through the final state interaction of the scattered particles. The unusual large-N_c behavior of

[a] e-mail: ivashyn@kipt.kharkov.ua
[b] e-mail: korchin@kipt.kharkov.ua

scalar resonances was recently summarized in [17] (see also references therein and the original paper [18]).

The decays $f_0/a_0(980) \to \gamma\,\rho(770)/\omega(782)$ are similar to the decays $\phi \to \gamma a_0$ (γf_0). The interest in these processes was initiated in [19]. Apparently they can be explained in terms of the same matrix element (describing a process with vector (V) and scalar (S) particles, and a photon in the initial/final state) with SU(3) flavor modifications reflecting the type of vector particles. The decays $S \to \gamma V$ may be studied experimentally in Jülich (with ANKE and WASA at COSY) [20] and possibly in Frascati [21] (with KLOE at DAΦNE or its upgrade) and at BES.

Various phenomenological models [5, 6, 12–14, 22–24] have been applied to the calculation of these decays. At the same time a consistent description in the framework of chiral perturbation theory (ChPT) with pre-existing vector and axial-vector mesons [25] is lacking. This is an effective theory of the strong and electromagnetic interactions at energies below 1 GeV, and it has the symmetries of the underlying QCD. Strictly speaking ChPT is a series expansion in $p^2/\Lambda_\chi^2, m^2/\Lambda_\chi^2$, where p is the momentum, m is the mass of the pseudoscalar mesons, and the chiral symmetry breaking scale Λ_χ is of order 1 GeV. Thus, formally, the range of energies for the scalar mesons is on the border of the applicability of ChPT. Nevertheless, it is clear that a suitable effective Lagrangian for scalar mesons has to have much in common with the ChPT Lagrangian, because the coupling structures are guided by the chiral symmetry. There are many successful applications of this theory at energies about 1 GeV that are a useful background for employing ChPT in the present problem.

In general, ChPT does not specify the internal structure of the interacting particles. The model [25] only assumes that the scalar fields belong to a SU(3) flavor octet and singlet. This Lagrangian is written down in Appendices A and B; in particular, $L^{\rm A}$ describes the interaction of pseudoscalar and vector mesons, and $L^{\rm B}$ the interaction of scalar mesons with pseudoscalars. We test the singlet–octet mixing scheme for the lightest scalar meson nonet

$$\begin{cases} a_0 &= S_3\,, \\ f_0 &= S^{\rm sing}\cos\theta - S_8\sin\theta\,, \\ \sigma &= S^{\rm sing}\sin\theta + S_8\cos\theta\,, \end{cases} \qquad (1)$$

where S_3 is the neutral isospin-one, S_8 is the isospin-zero member of the flavor octet and $S^{\rm sing}$ is the flavor singlet. θ is the octet–singlet mixing angle, and $\sigma = f_0(600)$. In particular, we are interested in whether $a_0(980)$ and $f_0(980)$ suit for members of this nonet. In principle, this may not be the case (see, for example, the argumentation in [26]), and it therefore should be verified. Radiative decays may help to clarify this important issue.

The present paper considers the decays $S \to \gamma\gamma$, $\phi(1020) \to \gamma S$ and $S \to \gamma V$. We assume that the underlying dynamics of all the above decays has much in common, namely that the loops with pseudoscalar mesons form the dominant mechanism. This assumption is consistently implemented in the Lagrangian [25], and Sect. 2 presents a calculation of the decay amplitudes. We prove cancellation of divergences and gauge invariance of the amplitudes. Along the calculations we use the dimensional regularization method; see Appendix D for a brief overview of the method and a list of the basic formulae. Some details of the calculation of the loop integrals and their analysis are also presented in Sect. 2.

There are six coupling constants in the Lagrangian (F_V, G_V, c_d, c_m, $\tilde{c}_d$ and $\tilde{c}_m$), and an estimation of their values is carried out in Sect. 3. Under the assumption of resonance saturation, the coupling constants may be expressed in terms of chiral LECs [25]. The available experimental data provide certain constraints on these couplings.

After fixing the parameters we calculate the widths of various decays with light scalar mesons and compare them with the available data and predictions of other models (Sect. 3). We compare pion- and kaon-loop contributions to the decays with the f_0 meson in the initial/final state and demonstrate the importance of pion loops in $f_0 \to \gamma\rho$ and $f_0 \to \gamma\gamma$ decays.

The virtual photon case, which is important for further applications of the present model, is outlined in Appendix C.

2 Formalism for radiative decays amplitudes

2.1 One-loop diagrams and chiral counting

From the Lagrangian terms (A.1) and (B.4) one obtains the sets of one-loop diagrams shown in Figs. 1, 2 and 3. In the present approach we have no tree-level diagrams for the radiative processes. Therefore the lowest-order amplitudes consist of one-loop diagrams. The corresponding set of diagrams for $a_0/f_0 \to \gamma\gamma$ decay with a pseudoscalar meson in the loop is shown in Fig. 1. This set of diagrams is complete, since it is obtained from a Lagrangian that carries a chiral power not less than the chiral power of any diagram.

The following rules [27] are used to count the chiral power of any diagram. These counting rules provide one with a guiding idea of which diagrams should be included and which should not, when forming a set of relevant diagrams at any given order. Pseudoscalar fields Φ, scalar fields S and vector fields (in the tensor representation) $\rho_{\mu\nu}$, $\omega_{\mu\nu}$ and $\phi_{\mu\nu}$ carry a zero chiral power $\mathcal{O}(p^0)$; a derivative or external source (like an electromagnetic field B_μ) has a unit chiral power $\mathcal{O}(p)$; the pseudoscalar-meson mass (m_π, m_K) also carries a unit power $\mathcal{O}(p)$ (so that the mass matrix χ in Appendix A is $\mathcal{O}(p^2)$). The propagator of the pseudoscalar meson is counted as $\mathcal{O}(p^{-2})$.

All coupling constants in the Lagrangian (c_d, c_m, $\tilde{c}_d$, $\tilde{c}_m$, F_V and G_V) are $\mathcal{O}(p^0)$, and the power of any vertex is determined only by the structure of the corresponding term in the Lagrangian. In addition, the loop integration over particle momentum adds $\mathcal{O}(p^4)$. Applying these rules one can show that each diagram in Figs. 1–3 has a chiral power $\mathcal{O}(p^4)$.

2.2 Radiative decays $a_0/f_0 \to \gamma\gamma$

Consider the amplitude of the decay $a_0/f_0 \to \gamma\gamma$. Let the scalar meson have 4-momentum p, and let the photons

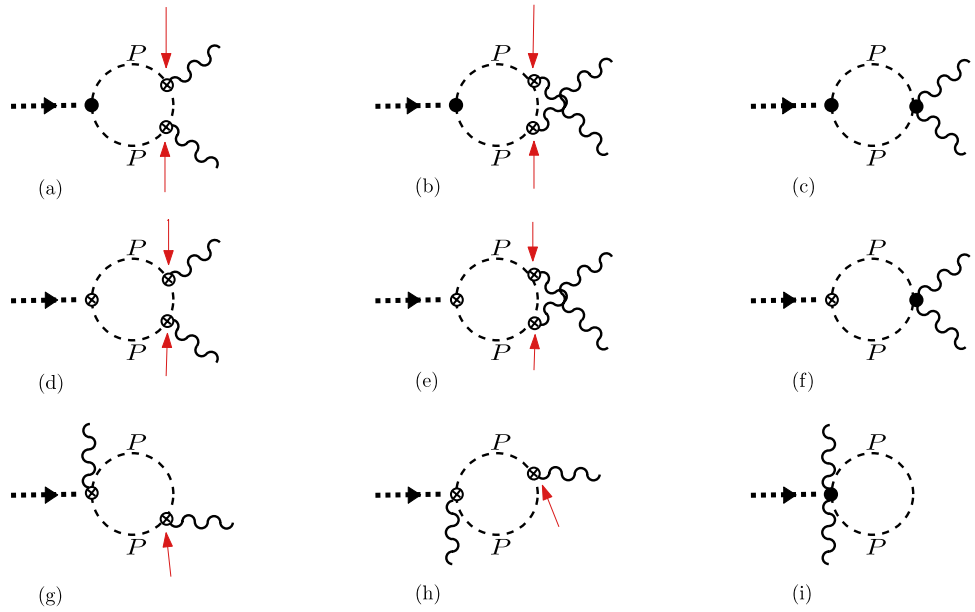

Fig. 1. Diagrams for the decay of the scalar meson (*dotted line*) into two photons (*wavy lines*). Pseudoscalar mesons (*dashed lines*) in the loops are (K^+K^-) for the $a_0(980)$ decays, and (K^+K^-), $(\pi^+\pi^-)$ for the $f_0(980)$ decays. *Solid* (non-derivative coupling) and *crossed* (derivative coupling) *blobs* represent $\mathcal{O}(p^2)$ vertices. *Arrows* mark the places where form factors of pion and kaon would arise for virtual photons (see discussion in Appendix C)

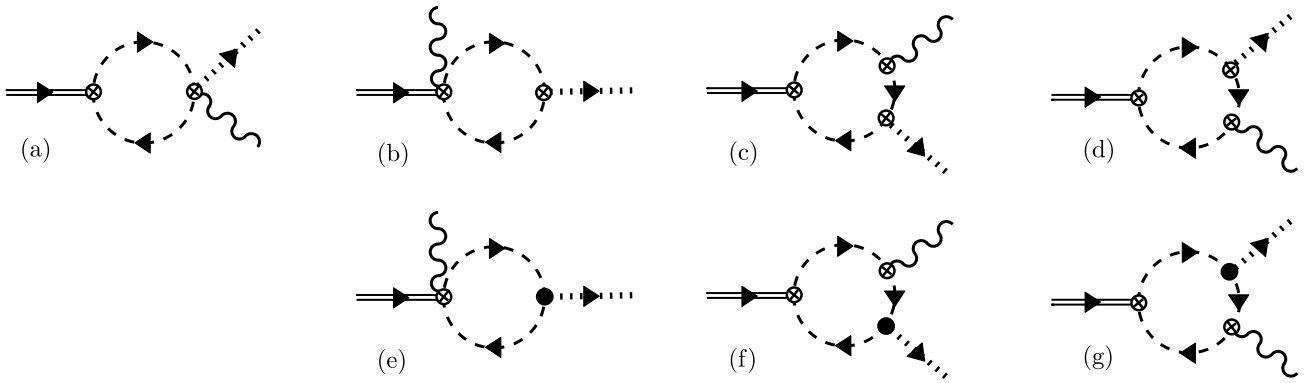

Fig. 2. Diagrams for the $\phi(1020)$ to $\gamma a_0(980)$ or $\gamma f_0(980)$ decays. Pseudoscalar mesons here are (K^+K^-). *Solid* and *crossed blobs* stand for $\mathcal{O}(p^2)$ vertices; the latter indicate derivative coupling terms

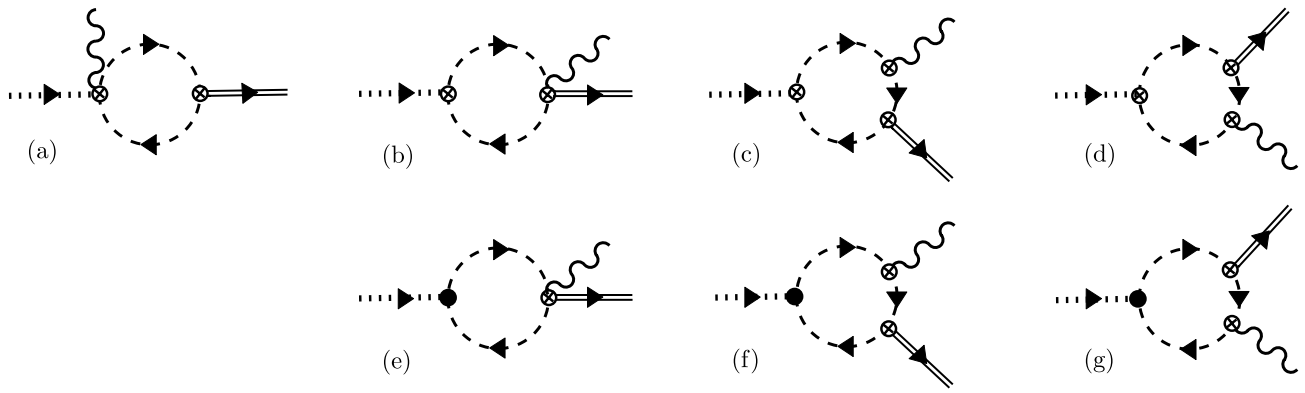

Fig. 3. Diagrams for $f_0(980)/a_0(980) \to \gamma\rho(770)/\omega(782)$ decays. The pseudoscalar mesons in the loops are (K^+K^-) for all decays, and $(\pi^+\pi^-,\ K^+K^-)$ for $f_0(980) \to \gamma\rho(770)$. *Solid* and *crossed blobs* stand for $\mathcal{O}(p^2)$ vertices; the latter are derivative coupling terms

have polarization vectors $\epsilon_\mu^{(1)}$ and $\epsilon_\nu^{(2)}$, and 4-momenta q_1^μ and q_2^ν. Suppose that a positive charge runs clockwise in the loop. First, we write down the amplitude for the first three diagrams (a–c), as this set of diagrams is often used in various approaches for radiative decays [5, 6, 19].

The invariant amplitude $\mathcal{M}_{\rm abc}$ corresponding to diagrams (Fig. 1a–c) is expressed through the tensor $T^{\mu\nu}_{S(P)\gamma\gamma}$:

$$-\mathrm{i}\mathcal{M}_{\rm abc} = \epsilon_\mu^{(1)*}\epsilon_\nu^{(2)*}T^{\mu\nu}_{S(P)\gamma\gamma}. \tag{2}$$

The indices $S(P)$ indicate that the scalar meson of type S decays in two photons via a loop consisting of two intermediate pseudoscalar mesons of type P with mass m_P, i.e. $S(P) = \{a_0(KK), f_0(KK), f_0(\pi\pi)\}$.

Explicitly, we find

$$\begin{aligned} T^{\mu\nu}_{S(P)\gamma\gamma} = &-\frac{e^2 g_{SPP}}{f_\pi^2}\left\{2g^{\mu\nu}\int\frac{\mathrm{d}^4 l}{(2\pi)^4}\Delta_l\Delta_{l-p}\right. \\ &\left. + I^{\nu\mu}(q_1,q_2) + I^{\mu\nu}(q_2,q_1)\right\}, \end{aligned} \tag{3}$$

$$\begin{aligned} I^{\nu\mu}(q_1,q_2) \equiv &\int\frac{\mathrm{d}^4 l}{(2\pi)^4}(2l-p-q_1)^\nu(2l-q_1)^\mu \\ &\times \mathrm{i}\Delta_l\Delta_{l-p}\Delta_{l-q_1}, \end{aligned}$$

where $\Delta_l \equiv \mathrm{i}(l^2-m_P^2)^{-1}$. For the g_{SPP} we refer to the Lagrangian (B.4) in Appendix B. Changing the integration variable $l' = p-l$ (and $l' = p+q_1-l$) and assuming that the possible divergence of the integrals is not higher than logarithmic, one can prove the gauge invariance of the amplitude:

$$q_{1\mu}T^{\mu\nu}_{S(P)\gamma\gamma} = q_{2\nu}T^{\mu\nu}_{S(P)\gamma\gamma} = 0\,. \tag{4}$$

Making use of the change $l' = p-l$ we deduce a useful relation:

$$I^{\nu\mu}(q_1,q_2) = I^{\mu\nu}(q_2,q_1)\,, \tag{5}$$

which is connected with Bose symmetry of the final photons.

By means of Feynman parametrization and the dimensional regularization method (see Appendix D) the expression (3) is reduced to

$$\begin{aligned} T^{\mu\nu}_{S(P)\gamma\gamma} = \frac{-2\mathrm{i}e^2}{(4\pi)^2}\frac{g_{SPP}}{f_\pi^2}&\left\{g^{\mu\nu}\int_0^1\mathrm{d}x\ln\left[m_P^2 - p^2x(1-x)\right]\right. \\ &- 2g^{\mu\nu}\iint_0^1 x\,\mathrm{d}x\,\mathrm{d}y\ln[C(x,y;q_1,q_2)] \\ &\left. - \iint_0^1 x\,\mathrm{d}x\,\mathrm{d}y\frac{A^{\nu\mu}(x,y;q_1,q_2)}{C(x,y;q_1,q_2)}\right\}, \end{aligned} \tag{6}$$

$$\begin{aligned} A^{\nu\mu}(x,y;q_1,q_2) &= (q_1[2x(1-y)-2] + 2xyp - q_2)^\nu \\ &\quad\times(q_1[2x(1-y)-1] + 2xy\,p)^\mu\,, \\ C(x,y;q_1,q_2) &= q_1^2x(x-1)(1-y) + p^2xy(x-1) \\ &\quad - q_2^2x^2y(1-y) + m^2\,. \end{aligned}$$

The divergent parts of diagrams (Fig. 1a–c) cancel each other.

For the real photons in question, we have

$$\begin{aligned} q_1^2 = q_2^2 = 0\,, \\ \epsilon_\mu^{(1)}q_1^\mu = \epsilon_\mu^{(2)}q_2^\mu = 0\,. \end{aligned}$$

These conditions simplify (6) to

$$T^{\mu\nu}_{S(P)\gamma\gamma} = \frac{-4\mathrm{i}e^2}{(4\pi)^2}\frac{g_{SPP}}{f_\pi^2}\left(g^{\mu\nu} - \frac{q_1^\nu q_2^\mu}{q_1\cdot q_2}\right)\Psi\left(m_P^2;p^2;0\right). \tag{7}$$

Here we define

$$\begin{aligned} \Psi\left(m_P^2;p^2;0\right) &\equiv \iint_0^1 x\,\mathrm{d}x\,\mathrm{d}y\left[1+\frac{m_P^2}{p^2xy(x-1)}\right]^{-1} \\ &= \frac{1}{2} - \frac{m_P^2}{p^2}\int_0^1\frac{\mathrm{d}x}{x-1}\ln\left[1+x(x-1)\frac{p^2}{m_P^2}\right], \end{aligned} \tag{8}$$

$$\mathrm{Re}\,\Psi\left(m_P^2;p^2;0\right) = \frac{1}{2} - \frac{m_P^2}{p^2}\int_0^1\frac{\mathrm{d}x}{x-1}\ln\left|1+x(x-1)\frac{p^2}{m_P^2}\right|,$$

$$\mathrm{Im}\,\Psi\left(m_\pi^2;p^2;0\right) = \pi\frac{m_\pi^2}{p^2}\ln\left|\frac{1+\sqrt{1-4\frac{m_\pi^2}{p^2}}}{1-\sqrt{1-4\frac{m_\pi^2}{p^2}}}\right|,$$

$$\mathrm{Im}\,\Psi\left(m_K^2;p^2;0\right) = 0\,.$$

The integrals $\Psi\left(m_P^2;p^2;0\right)$ are calculated numerically and presented in Table 1. The scalar-meson invariant mass

Table 1. Values of the loop integrals. The assumed physical values of the scalar meson masses are $M_{f_0} = 980$ MeV and $M_{a_0} = 984.7$ MeV

$\Psi\left(m_K^2;M_{a_0}^2;M_\phi^2\right)$	=	$0.0749 + 0.244\mathrm{i}$
$\Psi\left(m_K^2;M_{f_0}^2;M_\phi^2\right)$	=	$0.1295 + 0.216\mathrm{i}$
$\Psi\left(m_\pi^2;M_{a_0}^2;0\right)$	=	$0.5510 - 0.244\mathrm{i}$
$\Psi\left(m_K^2;M_{a_0}^2;0\right)$	=	-0.63
$\Psi\left(m_\pi^2;M_{f_0}^2;0\right)$	=	$0.5507 - 0.246\mathrm{i}$
$\Psi\left(m_K^2;M_{f_0}^2;0\right)$	=	-0.57
$\Psi\left(m_\pi^2;M_\sigma^2;0\right)$	=	$0.3545 - 0.5664\mathrm{i}$
$\Psi\left(m_K^2;M_\sigma^2;0\right)$	=	-0.0529
$\Psi\left(m_\pi^2;M_{f_0}^2;M_\rho^2\right)$	=	$0.128 - 0.0169\mathrm{i}$
$\Psi\left(m_K^2;M_{a_0}^2;M_\rho^2\right)$	=	-0.4048
$\Psi\left(m_K^2;M_{a_0}^2;M_\omega^2\right)$	=	-0.3988
$\Psi\left(m_K^2;M_{f_0}^2;M_\rho^2\right)$	=	-0.3466
$\Psi\left(m_K^2;M_{f_0}^2;M_\omega^2\right)$	=	-0.3407

$(p^2)^{1/2}$ is equal to M_s – the mass of f_0, a_0 (and σ for completeness), while m_P is equal to the mass of the pseudoscalar meson π or K in the loop.[1]

Now we consider the diagrams in Fig. 1d–i. At first glance, these diagrams, which include a derivative coupling for scalar mesons,[2] are more complicated due to momentum dependence of the SPP vertex. In fact, these diagrams can be treated similar to the previous case. To demonstrate this let us define

$$-\mathrm{i}\mathcal{M}_{(\mathrm{d\text{–}i})} = \epsilon_\mu^{(1)}\epsilon_\nu^{(2)}\hat{T}^{\mu\nu}_{S(P)\gamma\gamma}\,, \tag{9}$$

where the symbol "hat" is used hereafter to indicate the derivative coupling. Next we use the identity

$$l(l-p)\Delta_l\Delta_{l-p} = \frac{\mathrm{i}}{2}\left(\Delta_l + \Delta_{l-p} + \mathrm{i}(p^2-2m_P^2)\Delta_l\Delta_{l-p}\right),$$

and change the integration variables as above in order to combine the six terms in $\mathcal{M}_{(\mathrm{d\text{–}i})}$ in such a way that the contribution of diagram (i) cancels the contribution of (f), and diagrams (g) and (h) are cancelled by a part of (d) and a part of (e). In this way, the derivative coupling amplitude $\hat{T}^{\mu\nu}_{S(P)\gamma\gamma}$ is related to the non-derivative coupling amplitude $T^{\mu\nu}_{S(P)\gamma\gamma}$

$$\epsilon_\mu^{(1)}\epsilon_\nu^{(2)}\hat{T}^{\mu\nu}_{S(P)\gamma\gamma} = \frac{\hat{g}_{SPP}}{g_{SPP}}\left(m_P^2 - p^2/2\right)\epsilon_\mu^{(1)}\epsilon_\nu^{(2)}T^{\mu\nu}_{S(P)\gamma\gamma}\,.$$

Combining the contributions of all diagrams in Fig. 1, one obtains the total $\mathcal{O}(p^4)$ invariant amplitude

$$\begin{aligned}-\mathrm{i}\mathcal{M}_{a_0\to\gamma\gamma} = {}& \frac{-4\mathrm{i}e^2}{(4\pi)^2 f_\pi^2}\Psi\left(m_K^2;p^2;0\right)A_K\left(p^2\right)\\ &\times\left(\epsilon^{(1)*}\cdot\epsilon^{(2)*} - \frac{\epsilon^{(1)*}\cdot q_2\epsilon^{(2)*}\cdot q_1}{q_1\cdot q_2}\right),\end{aligned} \tag{10}$$

$$\begin{aligned}-\mathrm{i}\mathcal{M}_{f_0\to\gamma\gamma} = {}& \frac{-4\mathrm{i}e^2}{(4\pi)^2 f_\pi^2}\left[B_\pi(p^2)\Psi\left(m_\pi^2;p^2;0\right)\right.\\ &\left.+B_K(p^2)\Psi\left(m_K^2;p^2;0\right)\right]\\ &\times\left(\epsilon^{(1)*}\cdot\epsilon^{(2)*} - \frac{\epsilon^{(1)*}\cdot q_2\epsilon^{(2)*}\cdot q_1}{q_1\cdot q_2}\right),\end{aligned} \tag{11}$$

where

$$\begin{aligned}A_K(p^2) &\equiv \hat{g}_{aKK}(m_K^2 - p^2/2) + g_{aKK}\,,\\ B_K(p^2) &\equiv \hat{g}_{fKK}(m_K^2 - p^2/2) + g_{fKK}\,,\\ B_\pi(p^2) &\equiv \hat{g}_{f\pi\pi}(m_\pi^2 - p^2/2) + g_{f\pi\pi}\,.\end{aligned} \tag{12}$$

[1] When working with the integrals (8) it is convenient to use the identity $\int_0^1(1-2x)f(y)\,\mathrm{d}x = 0$ for any function $f(y)$, where $y = x(1-x)$.

[2] We also include here diagram (i), though it has no derivative coupling in the $SPP\gamma\gamma$ vertex. This is convenient due to its cancellation with the contribution of diagram (f).

2.3 Radiative decays $\phi(1020) \to \gamma a_0/f_0$

Let the vector meson $\phi(1020)$ with momentum Q decay into a scalar meson $a_0(980)$ (or $f_0(980)$) with momentum p and a photon with momentum q, i.e. $\phi(Q) \to \gamma(q) + a_0/f_0(p)$. Diagrams corresponding to these reactions are shown in Fig. 2.

Let the polarization vector for the ϕ-meson be E_μ, and that for the photon ϵ_ν. Apparently $q^\nu\epsilon_\nu = 0$ and $Q^\mu E_\mu = 0$. We describe the vector meson $\phi(1020)$ by the antisymmetric tensor field carrying the indices $\mu\lambda$. Thus we employ the normalization for the one-particle matrix element [25]

$$\langle 0|\phi_{\mu\lambda}(0)|\phi,Q\rangle = \mathrm{i}M_\phi^{-1}[Q_\mu E_\lambda - Q_\lambda E_\mu]\,. \tag{13}$$

The invariant amplitude reads

$$-\mathrm{i}\mathcal{M}_{\phi\to\gamma S} = \epsilon_\nu^*\mathrm{i}\frac{Q_\mu E_\lambda - Q_\lambda E_\mu}{M_\phi}\left(T^{\mu\lambda\nu}_{\phi\to\gamma S} + \hat{T}^{\mu\lambda\nu}_{\phi\to\gamma S}\right), \tag{14}$$

where the tensor with "hat" for the diagrams (a–d) in Fig. 2 is

$$\begin{aligned}\hat{T}^{\mu\lambda\nu}_{\phi\to\gamma S} &= \hat{T}^{\mu\lambda\nu}_{\mathrm{a}} + \hat{T}^{\mu\lambda\nu}_{\mathrm{b}} + \hat{T}^{\mu\lambda\nu}_{\mathrm{c}} + \hat{T}^{\mu\lambda\nu}_{\mathrm{d}}\,,\\ \hat{T}^{\mu\lambda\nu}_{\mathrm{a}} &= \frac{-\mathrm{i}eG_V\hat{g}_{SKK}}{\sqrt{2}f_\pi^4}\int\frac{\mathrm{d}^4l}{(2\pi)^4}\left(Q^\mu l^\lambda - (\mu\leftrightarrow\lambda)\right)\\ &\quad\times(2l-Q)^\nu\,\Delta_l\Delta_{l-Q}\,,\\ \hat{T}^{\mu\lambda\nu}_{\mathrm{b}} &= \frac{-\mathrm{i}e\hat{g}_{SKK}}{\sqrt{2}f_\pi^4}\int\frac{\mathrm{d}^4l}{(2\pi)^4}\\ &\quad\times\left[\left(G_V\,Q^\mu + \frac{1}{2}(F_V - 2\,G_V)q^\mu\right)g^{\nu\lambda} - (\mu\leftrightarrow\lambda)\right]\\ &\quad\times l\,(l-Q+q)\,\Delta_l\Delta_{l-Q+q}\,,\\ \hat{T}^{\mu\lambda\nu}_{\mathrm{c}} &= \hat{T}^{\mu\lambda\nu}_{\mathrm{d}}\\ &= \frac{eG_V\hat{g}_{SKK}}{\sqrt{2}f_\pi^4}\int\frac{\mathrm{d}^4l}{(2\pi)^4}\left(Q^\mu l^\lambda - (\mu\leftrightarrow\lambda)\right)\\ &\quad\times(2l-q)^\nu\,(l-q)(l-Q)\Delta_l\Delta_{l-q}\Delta_{l-Q}\,,\end{aligned} \tag{15}$$

and the tensor without "hat" for diagrams (e–g) in Fig. 2 reads

$$\begin{aligned}T^{\mu\lambda\nu}_{\phi\to\gamma S} &= T^{\mu\lambda\nu}_{\mathrm{e}} + T^{\mu\lambda\nu}_{\mathrm{f}} + T^{\mu\lambda\nu}_{\mathrm{g}}\,,\\ T^{\mu\lambda\nu}_{\mathrm{e}} &= \frac{-\mathrm{i}eg_{SKK}}{\sqrt{2}f_\pi^4}\int\frac{\mathrm{d}^4l}{(2\pi)^4}\Delta_l\Delta_{l-Q+q}\\ &\quad\times\left[g^{\nu\lambda}\left(G_VQ^\mu + \frac{1}{2}(F_V - 2G_V)q^\mu\right) - (\mu\leftrightarrow\lambda)\right],\\ T^{\mu\lambda\nu}_{\mathrm{f}} &= T^{\mu\lambda\nu}_{\mathrm{g}}\\ &= \frac{-eG_Vg_{SKK}}{\sqrt{2}f_\pi^4}\int\frac{\mathrm{d}^4l}{(2\pi)^4}\Delta_l\Delta_{l-q}\Delta_{l-Q}\,(2l-q)^\nu\\ &\quad\times\left(Q^\lambda l^\mu - (\mu\leftrightarrow\lambda)\right).\end{aligned} \tag{16}$$

The consideration shows that divergent parts of the amplitudes (15) and (16) that do not cancel are proportional to $(F_V - 2G_V)(g^{\nu\lambda}q^\mu - g^{\nu\mu}q^\lambda)$. Therefore, we employ the relation

$$F_V = 2G_V \tag{17}$$

between the electromagnetic and strong coupling constants of the vector mesons (see Appendix A) in order to make the amplitudes finite. Actually this relation does not follow from the chiral symmetry. However, it naturally appears in alternative approaches: the hidden local gauge symmetry model [28] and massive Yang–Mills theory [29]. This aspect has been addressed in [30]. In Appendix A we discuss the accuracy of (17) based on experiment.

Making use of (17) and the identities

$$\mathrm{i}(\Delta_{l-q}+\Delta_{l-Q}) = \Delta_{l-q}\Delta_{l-Q}\left[p^2-2m_K^2+2(l-q)(l-Q)\right],$$
$$\mathrm{i}(\Delta_{l}+\Delta_{l-Q+q}) = \Delta_{l}\Delta_{l-Q+q}\left[p^2-2m_K^2+2l(l-Q+q)\right]$$

in (15), one can prove that

$$\left(\hat{T}^{\mu\lambda\nu}_{\phi\to\gamma S}-\frac{\hat{g}_{SKK}}{g_{SKK}}\left(m_K^2-\frac{p^2}{2}\right)T^{\mu\lambda\nu}_{\phi\to\gamma S}\right)\times\epsilon^*_\nu \mathrm{i}\frac{Q_\mu E_\lambda - Q_\lambda E_\mu}{M_\phi}=0\,. \tag{18}$$

Finally,

$$-\mathrm{i}\mathcal{M}_{\phi\to\gamma S}=\left(1+\frac{\hat{g}_{SKK}}{g_{SKK}}\left(m_K^2-\frac{p^2}{2}\right)\right)\times T^{\mu\lambda\nu}_{\phi\to\gamma S}\epsilon^*_\nu \mathrm{i}\frac{Q_\mu E_\lambda - Q_\lambda E_\mu}{M_\phi}\,. \tag{19}$$

In the calculation of the amplitude, Feynman parametrization and the dimensional regularization method are applied (Appendix D). Then (19), with the use of (16), reads

$$-\mathrm{i}\mathcal{M}_{\phi\to\gamma S}=\frac{-\mathrm{i}eG_V g_{SKK}Q^2}{\sqrt{2}f_\pi^4(4\pi)^2M_\phi}\left(1+\frac{\hat{g}_{SKK}}{g_{SKK}}\left(m_K^2-\frac{p^2}{2}\right)\right)\times\left[4(Q\cdot\epsilon^*)(q\cdot E)I_1-(\epsilon^*\cdot E)(I_2-2I_3)\right], \tag{20}$$

where

$$I_2=\int_0^1 \mathrm{d}x\ln\left(m_K^2-p^2x(1-x)\right),$$
$$I_3=\iint_0^1 x\,\mathrm{d}x\,\mathrm{d}y \times\ln\left(m_K^2-Q^2x(1-x)+2xy(1-x)Q\cdot q\right),$$
$$I_1=\iint_0^1 x\,\mathrm{d}x\,\mathrm{d}y\frac{xy(1-x)}{m_K^2-Q^2x(1-x)+2xy(1-x)Q\cdot q}=\frac{1}{4Q\cdot q}\left(I_2-2I_3\right), \tag{21}$$
$$I_2-2I_3=1-\int_0^1\mathrm{d}x\frac{m_K^2-M_\phi^2x(1-x)}{(M_\phi^2-p^2)x(1-x)}\ln\frac{m_K^2-p^2x(1-x)}{m_K^2-M_\phi^2x(1-x)}\equiv 2\Psi\left(m_K^2,p^2,M_\phi^2\right). \tag{22}$$

In terms of $\Psi(m_K^2,p^2,M_\phi^2)$, the invariant amplitude (20) reads

$$-\mathrm{i}\mathcal{M}_{\phi\to\gamma S}=\mathrm{i}\frac{\sqrt{2}eM_\phi G_V}{f_\pi^4(4\pi)^2}2\Psi\left(m_K^2,p^2,M_\phi^2\right)\times\left[\epsilon^*\cdot E-\frac{1}{Q\cdot q}(Q\cdot\epsilon^*)(q\cdot E^*)\right]\times\begin{bmatrix}A_K(p^2) & \text{for} & \phi\to KK\to a_0\gamma\\ B_K(p^2) & \text{for} & \phi\to KK\to f_0\gamma\end{bmatrix}. \tag{23}$$

Compare definition (22) with that of $\Psi(m_P^2,p^2,0)$ in (8). The real and imaginary parts of $\Psi(m_K^2,p^2,M_\phi^2)$ at $p^2=M_s^2$ are

$$\mathrm{Re}\,\Psi\left(m_K^2,M_s^2,M_\phi^2\right)=\frac{1}{2}-\frac{1}{2}\int_0^1\mathrm{d}x\frac{m_K^2-M_\phi^2x(1-x)}{(M_\phi^2-M_s^2)x(1-x)}\ln\left|\frac{m_K^2-M_s^2x(1-x)}{m_K^2-M_\phi^2x(1-x)}\right|,$$
$$\mathrm{Im}\,\Psi\left(m_K^2,M_s^2,M_\phi^2\right)=\frac{\pi M_\phi^2}{M_\phi^2-M_s^2}\left(\sqrt{\frac{1}{4}-\frac{M_K^2}{M_\phi^2}}+\frac{M_K^2}{M_\phi^2}\ln\left|\frac{1-\sqrt{1-4\frac{M_K^2}{M_\phi^2}}}{1+\sqrt{1-4\frac{M_K^2}{M_\phi^2}}}\right|\right). \tag{24}$$

Numerical calculation of $\Psi(m_K^2,M_s^2,M_\phi^2)$ leads to the values shown in Table 1 (see also [5] for an analytic expression of the integral (22)).

2.4 Radiative decays $f_0/a_0\to\gamma\,\rho/\omega$

The decay of a scalar meson into a vector meson with radiation of a photon ($f_0/a_0\to\gamma\rho/\omega$) in the lowest order is represented by the $\mathcal{O}(p^4)$ diagrams shown in Fig. 3. The vertices follow from L^{A} in (A.1) and L^{B} in (B.4). The structure of the matrix element for these decays is very similar to that in (23). One can replace $\phi(1020)$ by $\rho(770)$ (or $\omega(782)$), take into account the flavor SU(3) factor in the VPP vertices, and select the pseudoscalar particles in the loops allowed by the symmetries of the strong interaction. For the relevant SU(3) relations, see Appendix A. Taking into account that $a_0(980)$ and $\omega(782)$ do not couple to two pions, one is left with K^+K^-, a loop for the $a_0\to\gamma V$ and $f_0\to\gamma\omega$ decays, and both the $\pi^+\pi^-$ and K^+K^- loops for the $f_0\to\gamma\rho$ decay.

The matrix elements read

$$-\mathrm{i}\mathcal{M}_{a_0\to\gamma V}=\frac{-\mathrm{i}eM_VG_V}{f_\pi^4(4\pi)^2}\left[\epsilon^*\cdot E^*-\frac{1}{Q\cdot q}(Q\cdot\epsilon^*)(q\cdot E^*)\right]\times 2A_K(p^2)\Psi\left(m_K^2;p^2;M_V^2\right), \tag{25}$$
$$-\mathrm{i}\mathcal{M}_{f_0\to\gamma\rho}=\frac{-\mathrm{i}eM_\rho G_V}{f_\pi^4(4\pi)^2}\left[\epsilon^*\cdot E^*-\frac{1}{Q\cdot q}(Q\cdot\epsilon^*)(q\cdot E^*)\right]\times 2\left(B_K(p^2)\Psi\left(m_K^2;p^2;M_\rho^2\right)+2B_\pi(p^2)\Psi\left(m_\pi^2;p^2;M_\rho^2\right)\right), \tag{26}$$

$$-\mathrm{i}\mathcal{M}_{f_0\to\gamma\omega} = \frac{-\mathrm{i}eM_\omega G_V}{f_\pi^4(4\pi)^2}\left[\epsilon^*\cdot E^* - \frac{1}{Q\cdot q}(Q\cdot\epsilon^*)(q\cdot E^*)\right] \times 2B_K(p^2)\Psi\left(m_K^2;p^2;M_\omega^2\right), \quad (27)$$

where the notation for the momenta and the polarization vectors is the same as in Sect. 2.3.

The loop integrals $\Psi\left(m_\pi^2;p^2;M_V^2\right)$ and $\Psi\left(m_K^2;p^2;M_V^2\right)$ can also be defined by (22). Their numerical values are shown in Table 1.

To establish correspondence with the results of [22] we can write the loop integrals for the $f_0/a_0\to\gamma\rho/\omega$ diagrams in Fig. 3 in the form

$$\mathrm{Re}\,\Psi\left(m_\pi^2;M_s^2;M_\rho^2\right) = \frac{1}{2} - \frac{1}{a-b} \times\left(\ln^2\frac{1+\sqrt{1-4/b}}{1-\sqrt{1-4/b}} - \ln^2\frac{1+\sqrt{1-4/a}}{1-\sqrt{1-4/a}}\right) + \frac{a}{2(a-b)}\left(\sqrt{1-4/b}\ln\frac{1+\sqrt{1-4/b}}{1-\sqrt{1-4/b}} - \sqrt{1-4/a}\ln\frac{1+\sqrt{1-4/a}}{1-\sqrt{1-4/a}}\right), \quad (28)$$

$$\mathrm{Im}\,\Psi\left(m_\pi^2;M_s^2;M_\rho^2\right) = \frac{\pi}{a-b} \times\left(\ln\frac{1+\sqrt{1-4/b}}{1-\sqrt{1-4/b}} - \ln\frac{1+\sqrt{1-4/a}}{1-\sqrt{1-4/a}}\right) - \frac{\pi a}{2(a-b)}\left(\sqrt{1-4/b} - \sqrt{1-4/a}\right), \quad (29)$$

with $a = M_\rho^2/m_\pi^2$ and $b = M_s^2/m_\pi^2$ for the pions in the loop. For the kaons in the loop, one finds

$$\Psi\left(m_K^2;M_s^2;M_V^2\right) = \frac{1}{2} + \frac{1}{a-b}\left(\arcsin^2\frac{\sqrt{b}}{2} - \arcsin^2\frac{\sqrt{a}}{2}\right) + \frac{a}{a-b}\left(\sqrt{4/b-1}\arcsin^2\frac{\sqrt{b}}{2} - \sqrt{4/a-1}\arcsin^2\frac{\sqrt{a}}{2}\right), \quad (30)$$

where $a = M_V^2/m_K^2$ and $b = M_s^2/m_K^2$. The numerical values obtained from these analytic expressions agree with those in Table 1 obtained from direct numerical integration. For the integrals (8) and (22) one can also deduce analytic expressions from [22] by choosing the appropriate a and b.

3 Results and discussion

3.1 Widths and estimates for chiral couplings

First of all there are direct decays, which can be described from (B.4) at tree level. They represent the dominant channels: $a_0\to\pi\eta$ for isotriplet and $f_0\to\pi\pi$ for isosinglet scalar mesons; we have

$$\Gamma_{a_0\to\pi\eta} = \frac{1}{8\pi p^2}\sqrt{\frac{\left(p^2+m_\pi^2-m_\eta^2\right)^2}{4p^2} - m_\pi^2}\frac{\left|A_{\pi\eta}(p^2)\right|^2}{f_\pi^4}, \quad (31)$$

$$\Gamma_{f_0\to\pi\pi} = \left(1+\frac{1}{2}\right)\frac{1}{8\pi p^2}\sqrt{p^2/4-m_\pi^2}\frac{1}{f_\pi^4}\left|B_\pi(p^2)\right|^2; \quad (32)$$

here $A_{\pi\eta}(p^2)$ is introduced by analogy with (12)

$$A_{\pi\eta}(p^2) \equiv \hat{g}_{a\pi\eta}\left(m_\eta^2+m_\pi^2-p^2\right)/2 + g_{a\pi\eta}, \quad (33)$$

and for the decays $a_0\to K\bar{K}$ and $f_0\to K\bar{K}$ we have

$$\Gamma_{a_0\to K\bar{K}} = 2\frac{1}{8\pi p^2}\sqrt{p^2/4-m_K^2}\frac{1}{f_\pi^4}\left|A_K(p^2)\right|^2, \quad (34)$$

$$\Gamma_{f_0\to K\bar{K}} = 2\frac{1}{8\pi p^2}\sqrt{p^2/4-m_K^2}\frac{1}{f_\pi^4}\left|B_K(p^2)\right|^2. \quad (35)$$

The invariant mass of the scalar meson is $\sqrt{p^2}$.

For the decays into $K\bar{K}$ in (34) and (35) one includes the factor 2 (as $K\bar{K} = K^+K^-, K^0\bar{K}^0$), and $(1+1/2(2\times 1/2)^2) = 3/2$ for $\pi\pi$ in (32): 1 is from the charged pions, 1/2 is from the identity of the neutral pions, $(1/2)^2$ is because the neutral pions interact two times weaker than the charged ones ($\vec{\pi}^2 = \pi^0\pi^0 + 2\pi^+\pi^-$), and 2 is the symmetry factor in the vertex with two identical neutral pions.

The widths of our premium interest are built up of $A_K(p^2)$, $B_K(p^2)$ and $B_\pi(p^2)$ (12), the loop integrals Ψ and phase-space factors. Thus, through the relations (12), they depend on the Lagrangian couplings c_d, c_m, $\tilde{c}_d$ and $\tilde{c}_m$ and the singlet–octet mixing angle θ for the scalar mesons (see Appendix B).

The widths for the $a_0\to\gamma\gamma$ and $f_0\to\gamma\gamma$ decays read

$$\Gamma_{a_0\to\gamma\gamma} = \frac{1}{32\pi\sqrt{p^2}}\frac{e^4}{8\pi^4 f_\pi^4}\left|A_K(p^2)\Psi\left(m_K^2;p^2;0\right)\right|^2, \quad (36)$$

$$\Gamma_{f_0\to\gamma\gamma} = \frac{1}{32\pi\sqrt{p^2}}\frac{e^4}{8\pi^4 f_\pi^4}\left|B_K(p^2)\Psi\left(m_K^2;p^2;0\right) + B_\pi(p^2)\Psi\left(m_\pi^2;p^2;0\right)\right|^2. \quad (37)$$

In deriving (36) and (37) the formula for the width

$$\Gamma_{S\to\gamma\gamma} = 1/(2\times 16\pi M_s)\left|\mathcal{M}_{S\to\gamma\gamma}\right|^2 \quad (38)$$

is used, with the amplitude defined in (10) and (11), and there is a symmetry factor 1/2 for two identical photons in the final state. Further, the sum over the polarization states λ of the photon is performed using

$$\sum_{\lambda=\pm1}\epsilon_\mu^{(\lambda)}\epsilon_\nu^{(\lambda)*} \to -g_{\mu\nu}, \quad (39)$$

under the condition that the polarization vector is contracted with the conserved current.

Table 2. Particle properties (data from PDG [32]) that are needed in the calculations

Particle	$I^G(J^{PC})$	Mass (MeV)	Width (MeV)	Major hadronic decay channels
$a_0(980)$	$1^-(0^{++})$	984.7 ± 1.2	50–100	$\pi\eta$
$f_0(980)$	$0^+(0^{++})$	980 ± 10	40–100	$\pi\pi$
$\sigma = f_0(600)$	$0^+(0^{++})$ [32]	400–1000	600–1000	$\pi\pi$
$\sigma = f_0(600)$	$0^+(0^{++})$ [33, 34]	513 ± 32	335 ± 67	$\pi\pi$
$\pi^\pm$	$1^-(0^-)$	139.57018 ± 0.00035	mean life 2.6×10^{-8} s	
$K^\pm$	$1/2(0^-)$	493.677 ± 0.016	mean life 1.24×10^{-8} s	$\pi^\pm\pi^0$
$\phi(1020)$	$0^-(1^{--})$	1019 ± 0.019	4.26	K^+K^-, $K^0_{\rm L}K^0_{\rm S}$, $\rho\pi + 3\pi$

The widths for the $\phi(1020)$ meson decays are

$$\Gamma_{\phi\to\gamma a_0} = \frac{1}{4\pi M_\phi}\frac{2}{3}\left(1-\frac{p^2}{M_\phi^2}\right)\left[\frac{\sqrt{2}eM_\phi G_V}{f_\pi^4(4\pi)^2}\right]^2 \times \left|A_K(p^2)\Psi\left(m_K^2,p^2,M_\phi^2\right)\right|^2, \quad (40)$$

$$\Gamma_{\phi\to\gamma f_0} = \frac{1}{4\pi M_\phi}\frac{2}{3}\left(1-\frac{p^2}{M_\phi^2}\right)\left[\frac{\sqrt{2}eM_\phi G_V}{f_\pi^4(4\pi)^2}\right]^2 \times \left|B_K(p^2)\Psi\left(m_K^2,p^2,M_\phi^2\right)\right|^2. \quad (41)$$

Equations (40) and (41) are derived from the general expression

$$\Gamma_{\phi\to\gamma a_0/f_0} = \frac{\overline{|\mathcal{M}_{\phi\to\gamma S}|^2}}{16\pi M_\phi}\left(1-\frac{M_s^2}{M_\phi^2}\right), \quad (42)$$

with the assumption (17). The amplitude $\mathcal{M}_{\phi\to\gamma S}$ is given in (23). The factor of 2/3 in (40) and (41) comes from the sum over the photon polarizations and the average over the vector-meson polarizations λ by means of

$$\sum_{\lambda=0,\pm1} E_\mu^{(\lambda)} E_\nu^{(\lambda)*} = -g_{\mu\nu} + \frac{Q_\mu Q_\nu}{M_\phi^2}. \quad (43)$$

The widths for the scalar meson decay into a photon and a vector meson have the form

$$\Gamma_{a_0\to\gamma\rho/\omega} = \frac{1}{2\pi\sqrt{p^2}}\left(1-\frac{M_{\rho/\omega}^2}{p^2}\right)\left[\frac{eM_{\rho/\omega}G_V}{f_\pi^4(4\pi)^2}\right]^2 \times \left|A_K(p^2)\Psi\left(m_K^2,p^2,M_{\rho/\omega}^2\right)\right|^2, \quad (44)$$

$$\Gamma_{f_0\to\gamma\rho} = \frac{1}{2\pi\sqrt{p^2}}\left(1-\frac{M_\rho^2}{p^2}\right)\left[\frac{eM_\rho G_V}{f_\pi^4(4\pi)^2}\right]^2 \times \left|B_K(p^2)\Psi\left(m_K^2,p^2,M_\rho^2\right) + 2B_\pi(p^2)\Psi\left(m_\pi^2,p^2,M_\rho^2\right)\right|^2, \quad (45)$$

$$\Gamma_{f_0\to\gamma\omega} = \frac{1}{2\pi\sqrt{p^2}}\left(1-\frac{M_\omega^2}{p^2}\right)\left[\frac{eM_\omega G_V}{f_\pi^4(4\pi)^2}\right]^2 \times \left|B_K(p^2)\Psi\left(m_K^2,p^2,M_\omega^2\right)\right|^2. \quad (46)$$

Table 3. Decay data

$\frac{\Gamma_{\phi(1020)\to\gamma f_0}}{\Gamma_{\phi,\rm tot}} = (4.40 \pm 0.21)\times 10^{-4}$	[32]
$\frac{\Gamma_{\phi(1020)\to\gamma a_0}}{\Gamma_{\phi,\rm tot}} = (7.6 \pm 0.6)\times 10^{-5}$	[32]
$\frac{\Gamma_{\phi(1020)\to\gamma f_0}}{\Gamma_{\phi(1020)\to\gamma a_0}} = 6.1 \pm 0.6$	[32]
$\Gamma_{a_0\to\gamma\gamma} = 0.30 \pm 0.10$ keV	[32]
$\Gamma_{f_0\to\gamma\gamma} = 0.31^{+0.08}_{-0.11}$ keV	[32]
$\frac{\Gamma_{a_0\to\eta\pi}\Gamma_{a_0\to\gamma\gamma}}{\Gamma_{a_0,\rm tot}} = 0.24^{+0.08}_{-0.07}$ keV	[32]
$\Gamma_{f_0\to\pi\pi} = 34.2^{+22.7}_{-14.3}$ MeV	[31]
$\Gamma_{f_0\to\gamma\gamma} = 0.205^{+0.242}_{-0.2}$ keV	[31]

The expressions (44)–(46) follow from

$$\Gamma_{S\to\gamma V} = \frac{1}{16\pi M_s}\left(1-\frac{M_V^2}{M_s^2}\right)\overline{|\mathcal{M}_{S\to\gamma V}|^2}, \quad (47)$$

where the scalar meson mass is M_s, the vector-meson mass M_V, and the matrix element $\mathcal{M}$ is given in (25), (26) and (27), respectively.

Let us discuss the difficulties one faces when trying to use (31)–(41) for fixing the couplings c_d, c_m, $\tilde{c}_d$ and $\tilde{c}_m$ and the mixing angle θ. It is clear that the accuracy and even the existence of the relevant experimental data are very important. The particle properties are presented in Table 2 and the known decay widths in Table 3 (the latter contains also very recent data from KEK [31]; however, the errors are still too large).

At present there is a big ambiguity in the mass of the $\sigma = f_0(600)$ meson [32] (although one notices smaller errors in the reference from CLEO [33, 34] in the 4th line in Table 2, given for overview purposes only). For that reason we decided not to use information on $\sigma = f_0(600)$ in the coupling estimation or in the prediction of the width.

Strictly speaking (34) and (35) are valid if the invariant mass of the scalar meson $\sqrt{p^2}$ is larger than the pair production threshold $2m_K$. In fact, the physical mass lies below threshold, i.e. $2m_K > M_{f_0}, M_{a_0}$ (Table 2). This makes it impossible to use (34) and (35) directly in the fitting procedure (in principle, one can use an approximate method [35]).

Table 4. Chiral couplings and mixing angle

B_π (10^7 MeV^3)	1.029	1.029	4.96	4.96
c_d (MeV)	-6.39	-52.57	-41.67	-264.37
c_m (MeV)	-58.83	-13.15	-23.93	196.37
θ (for $\mu=+1$)	-7.329°	46.271°	-7.329°	46.271°
θ (for $\mu=-1$)	-172.671°	133.729°	-172.671°	133.729°

From Table 3 one sees that the precision of the estimate for $\Gamma_{a_0\to\pi\eta}$ depends on the accuracy with which the total a_0 width $\Gamma_{a_0,\mathrm{tot}}$ is known, as only the ratio

$$\frac{\Gamma_{a_0\to\eta\pi}\Gamma_{a_0\to\gamma\gamma}}{\Gamma_{a_0,\mathrm{tot}}} \tag{48}$$

is measured [32]. Unfortunately, $\Gamma_{a_0,\mathrm{tot}}$ has a large experimental error and therefore extraction of $\Gamma_{a_0\to\pi\eta}$ from (48) leads to a large error. Thus, this information should not be used in the analysis.

Furthermore, formally (36) and (40) are not independent as they are expressed through the same factor A_K. We prefer to use (36), because of the non-trivial assumption (17) for the couplings used in the derivation of (40). For realistic values of F_V and G_V the relation (17) is satisfied only approximately (see Appendix A).

From the above reasoning, it becomes clear that fixing the five parameters in question is not an easy task. Therefore, we reduce the number of independent parameters from five to three by applying the large-N_c relations (B.2). These relations are briefly discussed in Appendix B. Then to find the values of c_d, c_m and θ one can use (36), (37) and (41).

In the analysis below we take the masses of $a_0(980)$ and $f_0(980)$ equal and put $\sqrt{p^2}\approx 980\,\mathrm{MeV}$. Let A_K, B_K and B_π be our estimates for $A_K(M_{a_0}^2)$, $B_K(M_{f_0}^2)$ and $B_\pi(M_{f_0}^2)$. Applying the constraint (B.2) to (12), we find that the scalar mixing angle θ satisfies the equation

$$4\mu\cos\theta+\sqrt{2}\sin\theta=\sqrt{6}\frac{B_K}{A_K}\,, \tag{49}$$

where $\mu=\pm1$ stands for the two possible choices of sign in (B.2). For the coupling constants

$$\begin{aligned} c_d &= \frac{\sqrt{2}}{p^2\,(m_K^2-m_\pi^2)}\left(m_\pi^2 A_K - m_K^2 R B_\pi\right),\\ c_m &= \frac{-1}{\sqrt{2}p^2\,(m_K^2-m_\pi^2)}\\ &\quad\times\left(\left(p^2-2m_\pi^2\right)A_K-\left(p^2-2m_K^2\right)RB_\pi\right), \end{aligned} \tag{50}$$

where

$$R^{-1}\equiv\frac{B_K}{A_K}-\sqrt{3}\sin\theta\,. \tag{51}$$

The values of A_K, B_K and B_π in (12), extracted from (36), (37) and (41) and experiment are

$$\begin{aligned} B_K &\approx 3.4716\times10^7\,\mathrm{MeV}^3\,,\\ B_\pi &\approx (1.029\text{ or }4.96)\times10^7\,\mathrm{MeV}^3\,,\\ A_K &\approx 2.2456\times10^7\,\mathrm{MeV}^3\,, \end{aligned} \tag{52}$$

(here $\mathrm{Im}\,B_\pi\equiv0$ is assumed). Inserting these values in (49) and (50), one obtains the couplings and mixing angle in Table 4. The relation between the mixing angle θ for $\mu=+1$ and $\mu=-1$ is discussed in Appendix B.

3.2 Analysis of the loop integrals

Here we analyze the dependence of the loop integrals (8), (22), (28)–(30) on the scalar meson invariant mass. Firstly, such dependences are important for processes in which the off-shell scalar resonances enter, i.e. for any scalar meson production and its subsequent decay to $\gamma\gamma$ or $\gamma\rho/\omega$. Secondly, the masses of the a_0 and f_0 mesons have not yet been accurately established. New experimental results may considerably alter the existing values and it is important to know how results of an approach depend on the masses.

Notice that our definition of the loop integral Ψ automatically includes the loop kinematic factors, i.e. $\Psi=(a-b)I(a,b)$ in terms of an analytic approach [22]. The quantity $|\Psi|^2$ is convenient in the analysis of the loop contribution to the decay probabilities (10), (11), (23) and (25)–(27).

Figure 4 shows the dependence of $|\Psi|^2$ on the scalar-meson invariant mass. This figure does not include any possible interference effects between the pion and the kaon loops. From Fig. 4c one sees that the pion contribution to the $f_0\to\gamma\gamma$ decay turns out to be as large as the kaon one. The loop integrals crucially depend on the pseudoscalar threshold and the relation between the masses of the pseudoscalar and vector particles. Especially the dependences for the kaon loops are complex due to the proximity of the $K\bar K$ threshold. The two dotted vertical lines in Fig. 4 show the physical masses of the scalar mesons. It is seen that the kaon-loop contribution rapidly changes near the $K\bar K$ threshold in the vicinity of M_{a_0} (M_{f_0}); therefore, an error in the mass value may cause drastic changes in the $K\bar K$ contribution.

Note that similar loop integrals for $\phi\to\gamma a_0/f_0$ and $a_0/f_0\to\gamma\rho/\omega$ decays were analyzed before in [5, 19, 22]. In particular, the authors of [19] concluded that the pion loops gave a negligible contribution to the decays.

In this connection we stress that for any observable not only the loop integrals but also the couplings matter. Thus,

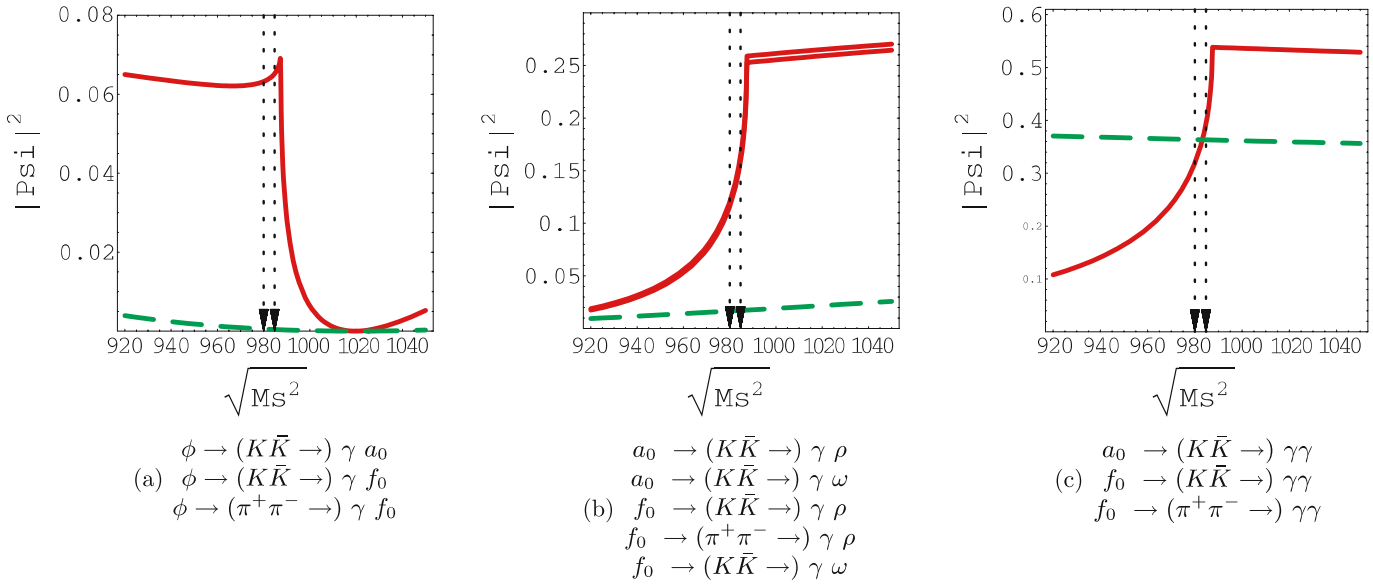

Fig. 4. Comparison of loop integrals squared, $|\Psi|^2$. *Solid line* is drawn for kaon loop, *dashed line* for pion loop. *Vertical dotted lines* mark assumed physical values of the scalar meson mass (M_{f_0} and M_{a_0}). The two *solid lines* in (**b**) account for the different masses of the ρ and ω mesons. Interference between kaon and pion loops is not included

it is important to compare the pion and kaon contributions taking into account the corresponding coupling constants as well as interference effects. Figure 5 shows the ratio of the $K\bar{K}$ contribution and the total $K\bar{K}+\pi\pi$ contribution calculated from (11), (26) and Table 1. This ratio exhibits the effect of interference between the pion and kaon loops and depends on the ratio B_K/B_π. Our estimates for the couplings lead to $B_K/B_\pi = 3.37$, and the arrows in Fig. 5 mark the values of the relative kaon contribution

$$\left|\frac{B_K\Psi\left(m_K^2, M_f^2, M_\rho^2\right)}{2\,B_\pi\Psi\left(m_\pi^2, M_f^2, M_\rho^2\right) + B_K\Psi\left(m_K^2, M_f^2, M_\rho^2\right)}\right|^2 = 1.635\,,$$

$$\left|\frac{B_K\Psi\left(m_K^2, M_f^2, 0\right)}{B_\pi\Psi\left(m_\pi^2, M_f^2, 0\right) + B_K\Psi\left(m_K^2, M_f^2, 0\right)}\right|^2 = 1.915\,,$$

to the decays $f_0 \to \gamma\rho$ and $f_0 \to \gamma\gamma$, respectively.

The results in Fig. 4a for the ϕ decays strongly favor the kaon loops compared to the pion loops. That would be an argument, additional to the OZI suppression rule, for not using pion loops for the ϕ decays. For other processes Fig. 5 gives an adequate measure of the pion–kaon concurrence. In $f_0 \to \gamma\rho$ decay omitting the pion loops would lead to a $\approx 60\%$ overestimate of the width. The pion loops are very important in the two-photon decay of f_0: they reduce the decay rate by a factor of 1.9.

3.3 Model predictions

In the present model two types of predictions are obtained. On the one hand, the observables depend on the values of the model parameters, and thus can be evaluated after specific values are chosen.

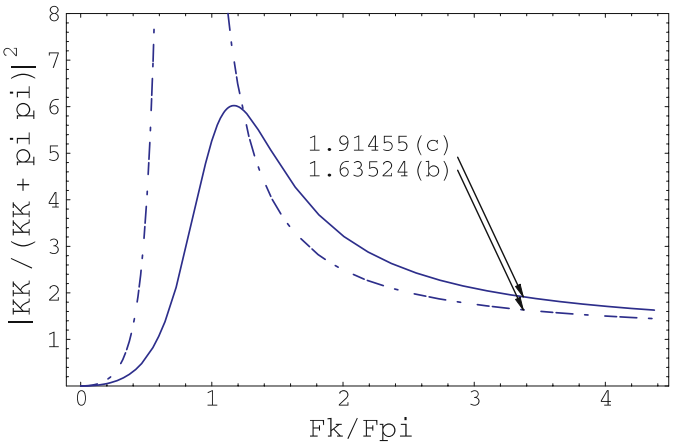

Fig. 5. Relative kaon loop contribution, $\left|(K\bar{K})/(\pi^+\pi^- + K\bar{K})\right|^2$, to (11) and (26) versus the ratio B_K/B_π. *Curves* (b) and (c) correspond to the decays $f_0 \to \gamma\rho$ and $f_0 \to \gamma\gamma$, respectively (see also the legend in Fig. 4). Our fit gives $B_K/B_\pi = 3.37$

On the other hand, several ratios of the widths turn out to be independent of specific values of the couplings c_m, c_d, $\tilde{c}_m$, $\tilde{c}_d$ and angle θ. We find three such ratios, which are constant in the present model for any values of these parameters:

$$\frac{\Gamma_{a_0\to\gamma\gamma}}{\Gamma_{\phi\to\gamma a_0}} = 0.422 = \frac{3e^2 f_\pi^4 M_\phi}{G_V^2 M_{a_0}\left(M_\phi^2 - M_{a_0}^2\right)}\left|\frac{\Psi\left(m_K^2; M_{a_0}^2; 0\right)}{\Psi\left(m_K^2; M_{a_0}^2; M_\phi^2\right)}\right|^2 . \quad (53)$$

Table 5. Strong decays of the scalar mesons

	Our estimate (I)	Estimate (II)	Estimate (III)	Exp. value [32]
c_d, MeV	-6.38	± 32	± 32	–
c_m, MeV	-58.83	± 42	± 42	–
θ	-7.33°	-35.26°	54.73°	–
$\Gamma_{a_0\to\pi\eta}$, MeV	14.2	172.4	172.4	–
$\Gamma_{f_0\to\pi\pi}$, MeV	41.8	775.7	7.4×10^{-6}	$34.2^{+22.7}_{-14.3}$
$\Gamma_{a_0,\mathrm{tot}}$, MeV	17.8	215.4	215.4	50–100

Table 6. Model predictions and available data for the electromagnetic decays. (An asterisk * marks the experimental values, used for the extraction of the couplings. For the couplings used in columns (I), (II) and (III), see Table 5)

Observable	Our est. (I)	Est. (II)	Est. (III)	[19] (IV)	[24] (Va)	[24] (Vb)	Exp. value [32]
$\frac{\Gamma_{\phi\to\gamma a_0}}{\Gamma_{\phi,\mathrm{tot}}}$, 10^{-4}	1.67	2.13	2.13	1.4	–	–	$(7.6\pm0.6)\times10^{-1}$
$\frac{\Gamma_{\phi\to\gamma f_0}}{\Gamma_{\phi,\mathrm{tot}}}$, 10^{-4}	4.40*	2.31	4.63	1.4	4.92 ± 0.07	4.92 ± 0.07	4.40 ± 0.21
$\frac{\Gamma_{\phi\to\gamma f_0}}{\Gamma_{\phi\to\gamma a_0}}$	2.64	1.08	2.17	1	0.26 ± 0.06	0.46 ± 0.09	6.1 ± 0.6
$\Gamma_{a_0\to\gamma\gamma}$, keV	0.30*	0.383	0.383	0.24	0.28 ± 0.09*	0.28 ± 0.09*	0.30 ± 10
$\Gamma_{f_0\to\gamma\gamma}$, keV	0.31*	0.323	0.62	0.24	0.39 ± 0.13*	0.39 ± 0.13*	$0.31^{+0.08}_{-0.07}$
$\Gamma_{a_0\to\gamma\rho}$, keV	9.1	11.65	11.65	3.4	3.0 ± 1.0	3.0 ± 1.0	–
$\Gamma_{f_0\to\gamma\rho}$, keV	9.6	0.95	16.6	3.4	19 ± 5	3.3 ± 2.0	–
$\Gamma_{a_0\to\gamma\omega}$, keV	8.7	11.15	11.15	3.4	641 ± 87	641 ± 87	–
$\Gamma_{f_0\to\gamma\omega}$, keV	15.0	7.93	15.85	3.4	126 ± 20	88 ± 17	–

From experiment (Table 3) one obtains about 0.93 for this ratio.

Another ratio,

$$\frac{\Gamma_{a_0\to\gamma\rho}}{\Gamma_{a_0\to\gamma\omega}} = 1.043 = \frac{\left(M_{a_0}^2-M_\rho^2\right)M_\rho^2}{\left(M_{a_0}^2-M_\omega^2\right)M_\omega^2}\left|\frac{\Psi\left(m_K^2;M_{a_0}^2;M_\rho^2\right)}{\Psi\left(m_K^2;M_{a_0}^2;M_\omega^2\right)}\right|^2, \tag{54}$$

has not been measured so far, though theoretical predictions exist. In particular, it was shown [19] that the quark-loop mechanism in the two-quark model gives a value of about 1/9, the four-quark structure leads to ≈ 0, while the kaon-loop mechanism produces almost equal $a_0\to\gamma\rho$ and $a_0\to\gamma\omega$ widths. Our result appears to be close to the latter prediction.

From (40) and (44) it is also possible to derive

$$\frac{\Gamma_{a_0\to\gamma\rho(\omega)}}{\Gamma_{\phi\to\gamma a_0}} \approx 12 = \frac{3M_\phi^3}{M_{a_0}^3}\frac{M_{a_0}^2-M_{\rho(\omega)}^2}{M_\phi^2-M_{a_0}^2}\left(\frac{M_{\rho(\omega)}^2}{2M_\phi^2}\right)\left|\frac{\Psi\left(m_K^2,M_{a_0}^2,M_{\rho(\omega)}^2\right)}{\Psi\left(m_K^2,M_{a_0}^2,M_\phi^2\right)}\right|^2. \tag{55}$$

The analogous ratio can be deduced from the results of [16]. It appears to be approximately 5.6. The difference may be caused by the dissimilarity between the models, in particular the choice of the mass and the coupling constant values.

Now, let us focus on the coupling-dependent results calculated according to (31), (32), (36), (37), (40), (41) and (44)–(46). Tables 5 and 6 show the predictions of the model and a comparison with the available data. Table 5 presents the values obtained for c_d, c_m and θ, and the strong decay widths for the a_0 and f_0 mesons.

In Table 6 one can see the results for the radiative decay widths. Column I shows the calculations with our parameters $c_d=-6.38\,\mathrm{MeV}$, $c_m=-58.83\,\mathrm{MeV}$ and $\theta=-7.33^\circ$. The entries in Table 6, which were taken as input in the fitting procedure, are marked with an asterisk ($\Gamma_{\phi\to\gamma f_0}/\Gamma_{\phi,\mathrm{tot}}$, $\Gamma_{a_0\to\gamma\gamma}$ and $\Gamma_{f_0\to\gamma\gamma}$). Column II is calculated with an "ideal" mixing angle $\theta=-35.3^\circ$ ($\sin\theta=-1/\sqrt{3}$, $\cos\theta=\sqrt{2/3}$) as chosen in [36]. In this case the decay $\sigma=f_0(600)\to\pi\pi$ is forbidden,[3] though in fact it should be super-allowed. Column III deals with another "ideal" mixing angle $\theta=54.7^\circ$ ($\cos\theta=1/\sqrt{3}$ and $\sin\theta=\sqrt{2/3}$). In this case the decay $f_0(980)\to\pi\pi$ turns out to be forbidden, in contradiction with experimental evidence. Therefore the choices II and III do not look realistic.

For comparison of our results with predictions of other models we add columns IV, Va and Vb. In particular, the kaon-loop model [19] (KLM) is selected (column IV), which is somewhat similar to the present calculation. In

[3] In the $q\bar{q}$ quark model this case corresponds to $f_0(600)=s\bar{s}$.

columns Va and Vb the predictions of the vector-meson-dominance (VMD) model [24] (Table I therein) are shown for two different sets of parameters. The authors apply a chiral Lagrangian with strong trilinear scalar–vector–vector interaction.

3.4 Discussion

In this subsection we briefly compare our results with those of the KLM [19] and VMD [24] models and comment on the correspondence of the predicted widths to experiment.

As is seen from Table 6, our model, contrary to KLM, gives not only the rate for the decay of a given type ($S \to \gamma\gamma$, $S \to \gamma V$ and $\phi \to \gamma S$ groups) but also different decay rates for the a_0 and f_0 mesons. For some of the channels the results of KLM are qualitative estimates, corrections [14] to which should be calculated as discussed in [19]. Nevertheless, our results for $S \to \gamma\gamma$ and $\phi \to \gamma S$ are in agreement with KLM within an order of magnitude. For the ratio $\Gamma_{a_0\to\gamma\gamma}/\Gamma_{\phi\to\gamma a_0}$ we also get a close value, which approximately corresponds to the experimental result. At the same time we obtain the widths for the $S \to \gamma V$ decays that are larger than the values in the KLM. The latter discrepancy is due to the SU(3) relations for the strong interaction (see (A.11)), and our couplings of the ϕ and ρ/ω mesons to $K\bar{K}$ turn out to be different from those used in [19].

Regarding the VMD model [24], one can see from Table 6 that quite big decay widths for $S \to \gamma\omega$ are obtained there compared to our results, while the $S \to \gamma\rho$ predictions differ not so much. Note also the large difference in the values of the ratio $\Gamma_{\phi\to\gamma f_0}/\Gamma_{\phi\to\gamma a_0}$.

From the results presented in Tables 5 and 6 one concludes that the predictions for the scalar meson decay widths are very sensitive to details of the model. Therefore, the future experiments in which these processes will be studied may help one to discriminate between different models of the scalar mesons.

In general, for comparison with experiment, in which scalar resonances contribute, a more appropriate observable is the invariant mass distribution. As an example consider the reaction $e^+e^- \to \gamma^* \to \pi\pi\gamma$ at the CM energy close to the $\phi(1020)$ mass [2]. This reaction allows for the extraction of the branching ratio:

$$\frac{\mathrm{d}B_{\phi\to\pi\pi\gamma}}{\mathrm{d}p^2} = \frac{1}{\Gamma_{\phi,\mathrm{tot}}}\frac{\mathrm{d}\Gamma_{\phi\to\pi\pi\gamma}}{\mathrm{d}p^2}\,, \tag{56}$$

where p^2 is the two-pion invariant mass squared. Within the present framework this branching ratio can be calculated from

$$\frac{\mathrm{d}\Gamma_{\phi\to\pi\pi\gamma}}{\mathrm{d}p^2} = \Gamma_{\phi\to\gamma f_0}\left(p^2\right) B_{f_0\to\pi\pi}\left(p^2\right)\left(-\frac{1}{\pi}\right)\mathrm{Im}\, D_{f_0}(p^2)\,. \tag{57}$$

Here $\Gamma_{\phi\to\gamma f_0}(p^2)$ is the $\phi \to \gamma f_0$ decay width (41) for arbitrary p^2, $D_{f_0}(p^2) = [p^2 - m_f^2 + \mathrm{i}m_f\Gamma_{f_0,\mathrm{tot}}(p^2)]^{-1}$ is the scalar-meson propagator and the branching ratio $B_{f_0\to\pi\pi}(p^2) = \Gamma_{f_0\to\pi\pi}(p^2)/\Gamma_{f_0,\mathrm{tot}}(p^2)$ relates the $f_0 \to \pi\pi$ decay width (32) to the total f_0 width $\Gamma_{f_0,\mathrm{tot}}(p^2)$. A more advanced form of the propagator including both real and imaginary parts of the self-energy was suggested recently [37]. The problem of finite resonance width effects in the invariant mass distributions for $\pi^0\pi^0$ and $\pi^0\eta$ in the ϕ radiative decays is important [38].

Note also that in [19] (in the appendix) a more general distribution over invariant masses of both the initial and final resonances for the $S \to \gamma V$ decays is discussed.

The scalar octet and singlet mixing angle θ appeared to be a crucial parameter in the fit. We should remark that a detailed study of the mixing angle was performed in [39] using the inverse amplitude method. The basic processes in this reference were elastic $\pi\pi$, $\pi\eta$, $K\bar{K}$ and $K\eta$ scattering and the value of the angle was different from our estimate.[4] There are also models in which f_0 is mainly the singlet state with $\theta \approx 0$; for example, an application of the Bethe–Salpeter equation with a linear confinement $q\bar{q}$ potential to the calculation of the scalar-meson mass spectrum [40].

These discrepancies, in our opinion, maybe are not caused only by differences in the applied models. The problem may be related to the non-trivial structure and behavior of the light scalar resonances. As was emphasized by Bugg [8], unification of the observed resonances in elastic scattering experiments with the corresponding ones seen in radiative decays is a big challenge. They show up in different ways, and it would be important to build a consistent bridge between these properties of the resonances.

3.5 Possible interactions beyond the model

Comparison of our results with predictions of other models, especially the results independent of the choice of the couplings, shows that the present model does not allow one to reproduce the ratio $\Gamma_{a_0\to\gamma\rho}/\Gamma_{a_0\to\gamma\omega} = 1/9$, which is obtained in the $q\bar{q}$ model and the quark-loop mechanism [19], or $\Gamma_{a_0\to\gamma\rho}/\Gamma_{a_0\to\gamma\omega} \approx 0$ in the $qq\bar{q}\bar{q}$ model [19]. The present model is insensitive to the structure of the scalars.

At this point one can think of a direct (or contact) coupling of the scalars to two photons as an extension of the present model. Similar terms were introduced in [36] and have the order $\mathcal{O}(p^4)$:

$$L_1 = g\left\langle S^{\mathrm{oct}} f_+^{\mu\nu} f_{+\mu\nu}\right\rangle + g' S^{\mathrm{sing}}\left\langle f_+^{\mu\nu} f_{+\mu\nu}\right\rangle\,, \tag{58}$$

where g and g' are coupling constants and $f_+^{\mu\nu}$ is defined in (A.6).

Analogously, constructing the C and P invariant terms with $V_{\mu\nu}$ one can propose the $S\gamma V$ interactions

$$L_2 = g''\left\langle S^{\mathrm{oct}} f_+^{\mu\nu} V_{\mu\nu}\right\rangle + g''' S^{\mathrm{sing}}\left\langle f_+^{\mu\nu} V_{\mu\nu}\right\rangle\,, \tag{59}$$

which are bilinear in the resonance fields. The Lagrangian (59) has the order $\mathcal{O}(p^2)$ and contains two more couplings g'' and g'''. Of course, these terms do not violate the chiral symmetry. The four additional coupling constants g, g', g'' and g''' should be fixed from certain observables.

[4] The definition of the mixing angle in [39] is also different.

In our opinion, the Lagrangians (58) and (59) can be useful in phenomenological descriptions of the scalar radiative decays. They may represent effects related to the specific quark structure of the scalar mesons, which is not accounted for in the chiral Lagrangian $L^{\rm B}$ of (B.1). This aspect lies beyond the scope of the present paper.

4 Conclusions

Within ChPT with vector and scalar mesons [25] we have calculated the radiative decays $a_0 \to \gamma\gamma$, $f_0 \to \gamma\gamma$, $\phi \to \gamma a_0$ and $\phi \to \gamma f_0$. These decays and the corresponding invariant mass distributions can be measured in e^+e^- annihilation in Frascati by KLOE [21, 41] and Novosibirsk with VEPP-2000.

The derivative and non-derivative couplings of the scalar mesons to the pseudoscalar ones are consistently included. The gauge invariance of the amplitudes and cancellation of the divergences from various diagrams are explicitly demonstrated. The amplitudes obtained are finite without counter terms. For the ϕ decays, in addition, we used the relation $F_V = 2G_V$ between the electromagnetic and strong couplings of the vector mesons in order to get rid of the divergences. This relation was previously discussed in [30] in connection with alternative approaches: hidden local gauge symmetry [28] and massive Yang–Mills models [29]. Note that this relation does not follow from chiral symmetry but does not contradict it either [30].

The scalar flavor singlet–octet mixing angle θ is obtained from the fit, as well as estimates for the octet chiral couplings c_m and c_d. It should be noted that the values of these parameters strongly correlate with the mixing angle.

For the flavor singlet couplings $\tilde{c}_{d,m}$ we relied on the relations $\tilde{c}_{d,m} = c_{d,m}/\sqrt{3}$ in the large-N_c limit [25]. One may argue on whether the large-N_c consideration is applicable to scalar mesons, especially in view of unitarized ChPT results [18]. In this connection, a fit without any large-N_c restriction would be an extension of the present approach. However, difficulties related to the fitting procedure may arise; in particular, two more free parameters $\tilde{c}_{d,m}$ appear, and in view of the scarce experimental data a non-trivial procedure is needed to reduce the ambiguities in the results.

In the present model we obtained the widths of the $a_0(980)$ and $f_0(980)$ decays: $\Gamma_{a_0,\rm tot} = 17.8\,\text{MeV}$, $\Gamma_{a_0\to\pi\eta} = 14.2\,\text{MeV}$ and $\Gamma_{f_0\to\pi\pi} = 41.8\,\text{MeV}$. Many of the calculated observables are in satisfactory agreement with experiment. At the same time the calculated ratio $\Gamma_{\phi\to\gamma f_0}/\Gamma_{\phi\to\gamma a_0} = 2.64$ only qualitatively agrees with the experimental value 6.1. The results of the present approach are also compared with those of the previously developed kaon-loop model [19] and the vector-meson-dominance model [24].

Predictions for the widths of the $a_0(980)$ and $f_0(980)$ decays into $\gamma\rho(770)$ and $\gamma\omega(782)$ are also given (see Table 6). The processes, to our opinion, are of interest for the experimental programs in Jülich with COSY [20] and Frascati with DAΦNE (or its upgrade) [42, 43].

Within the present model and the one-loop approximation, we found several ratios of the widths, which are independent of the couplings constants. Namely, $\Gamma_{a_0\to\gamma\gamma}/\Gamma_{\phi\to\gamma a_0} = 0.422$, which is in qualitative correspondence with experiment, and $\Gamma_{a_0\to\gamma\rho}/\Gamma_{a_0\to\gamma\omega} = 1.043$ and $\Gamma_{a_0\to\gamma\rho(\omega)}/\Gamma_{\phi\to\gamma a_0} \approx 12$, which have not been tested experimentally yet.

Our calculations show that many predictions are in agreement with experiment, and therefore support the assumption that $a_0(980)$ and $f_0(980)$ fit in the lightest scalar meson nonet. However, it is difficult to make an unambiguous conclusion.

The present work makes a solid ground for further studies of the scalar mesons, not only the lightest ones, $a_0(980)$ and $f_0(980)$. The model can be applied in processes of two-photon production of hadronic states with intermediate scalar resonances. These processes occur in nucleon–nucleon and electron–positron collisions (like $e^+e^- \to e^+e^-\pi^+\pi^-$).

Acknowledgements. We would like to thank N.P. Merenkov for reading the manuscript and for making useful remarks. We are also grateful to S. Eidelman for comments and suggestions, and to C. Hanhart and A. Nefediev for discussion. The suggestions kindly given by J.R. Peláez will help with further development of the approach. One of the authors (A.Y.K.) acknowledges support by the INTAS grant 05-1000008-8328 "Higher order effects in e^+e^- annihilation and muon anomalous magnetic moment". S.I. warmly acknowledges the hospitality of the A. Salam ICTP in Trieste, Italy, where a part of the article was prepared.

Appendix A: Chiral Lagrangian for pseudoscalar and vector mesons

In the calculations we use the $\mathcal{O}(p^2)$ ChPT Lagrangian for the pseudoscalar mesons Φ, and the vector mesons and photons, derived by Ecker et al. [25], where spin-1 mesons are described by antisymmetric tensor fields $V^{\nu\mu}$. This Lagrangian has a $\mathcal{O}(p^4)$ chiral power in the sense of its equivalence to the ChPT Lagrangian, in which no explicit resonances are introduced [25, 30]. In the present problem it is sufficient to keep

$$\begin{aligned} L^{\rm A} = {} & \frac{f_\pi^2}{4}\left\langle D_\mu U D^\mu U^\dagger + \chi U^\dagger + \chi^\dagger U\right\rangle - \frac{1}{4}F_{\mu\nu}F^{\mu\nu} \\ & - \frac{1}{2}\langle \nabla^\lambda V_{\lambda\mu}\nabla_\nu V^{\nu\mu} - \frac{1}{2}M_V^2 V_{\mu\nu}V^{\mu\nu}\rangle \\ & + \frac{F_V}{2\sqrt{2}}\left\langle V_{\mu\nu} f_+^{\mu\nu}\right\rangle + \frac{{\rm i}G_V}{\sqrt{2}}\left\langle V_{\mu\nu}u^\mu u^\nu\right\rangle , \end{aligned} \tag{A.1}$$

where $\langle\cdots\rangle$ stands for the trace in flavor space. The pion weak decay constant is $f_\pi \approx 92.4\,\text{MeV}$, and F_V and G_V are coupling constants. The electromagnetic field B^μ is included as an external source, and $F_{\mu\nu} = \partial_\mu B_\nu - \partial_\nu B_\mu$ is the electromagnetic field tensor. The quark mass matrix,

$$\chi = 2B_0 {\rm diag}(m_u, m_d, m_s)\,, \tag{A.2}$$

is expressed in terms of the light quark (q_u, q_d, q_s) masses and the chiral condensate: $\langle 0|\bar{q_u}q_u|0\rangle = -f_\pi^2 B_0\,(1+\mathcal{O}(m_q))$. In the limit of exact isospin symmetry $\chi = \mathrm{diag}\left(m_\pi^2, m_\pi^2, 2m_K^2 - m_\pi^2\right)$. The terms in the Lagrangian relevant for the scalar meson sector are discussed in Appendix B, and they are denoted as L^{B} in the present paper.

The pseudoscalar meson nonet ($J^P = 0^-$) contains the $\mathbf{8}_{\mathrm{flavor}}$ octet of Goldstone bosons and the $\mathbf{1}_{\mathrm{flavor}}$ singlet, namely the η_0 field. We combine singlet and octet into a nonet following [45, 46]. Thus the flavor SU(3) multiplet for the pseudoscalar mesons is

$$\begin{aligned}\Phi = \frac{1}{\sqrt{2}}(&\pi_1\lambda_1 + \pi_2\lambda_2 + \pi_3\lambda_3 + K_1\lambda_4 \\ &+ K_2\lambda_5 + K_3\lambda_6 + K_4\lambda_7 + \eta_8\lambda_8 + \eta_0\lambda_0)\,, \end{aligned} \quad (A.3)$$

where λ_a $(a = 1, ..., 8)$ are the Gell-Mann matrices, $\lambda_0 = \sqrt{\frac{2}{3}}\,1$, and the physical fields are defined as

$$\begin{aligned} \pi^\pm &= \frac{1}{\sqrt{2}}(\pi_1 \mp \mathrm{i}\pi_2)\,, \qquad K^\pm = \frac{1}{\sqrt{2}}(K_1 \mp \mathrm{i}K_2)\,, \\ K^0 &= \frac{1}{\sqrt{2}}(K_3 - \mathrm{i}K_4)\,, \qquad \bar{K^0} = \frac{1}{\sqrt{2}}(K_3 + \mathrm{i}K_4)\,, \\ \pi^0 &= \pi_3\,. \end{aligned} \quad (A.4)$$

Of course such a scheme is only approximately well defined if the U(1) axial anomaly is neglected. We do not omit the problematic η meson within the present approach, as it is involved in the dominant decay of the a_0 meson, $a_0 \to \pi\eta$. For η–η' mixing we choose the two-parameter scheme [47]:

$$\begin{aligned} \eta &= \cos\theta_8\eta_8 - \sin\theta_0\eta_0\,, \\ \eta' &= \sin\theta_8\eta_8 + \cos\theta_0\eta_0\,. \end{aligned} \quad (A.5)$$

Note that η and η' are not orthogonal states. The angles $\theta_0 = -9.2^\circ$ and $\theta_8 = -21.2^\circ$ are discussed and determined in [47, 48] from experiment.

Further, $f_+^{\mu\nu}$ in (A.1) for the external electromagnetic field reads

$$f_+^{\mu\nu} = eF^{\mu\nu}(uQu^+ + u^+Qu)\,, \quad (A.6)$$

where

$$u \equiv U^{1/2} = \exp\left(\frac{\mathrm{i}\Phi}{\sqrt{2}f_\pi}\right) \quad (A.7)$$

carries a non-linear parametrization of the pseudoscalar field. The quark charge matrix is

$$Q \equiv \mathrm{diag}\left(\frac{2}{3}, -\frac{1}{3}, -\frac{1}{3}\right) = \frac{1}{2}\lambda_3 + \frac{1}{2\sqrt{3}}\lambda_8\,,$$

and the electron charge is $e = \sqrt{4\pi\alpha} \approx 0.303$.

The definition of $D_\mu U$, $\nabla_\nu V^{\nu\mu}$ and u^ν in (A.1) can be found in the original work [25].

From L^{A} (A.1) the following interactions for the physical fields in order $\mathcal{O}(p^2)$ can be produced [44]:

$$\mathcal{L}_{\gamma PP} = -\mathrm{i}eB_\mu\left(\pi^+ \overset{\leftrightarrow}{\partial_\mu} \pi^- + K^+ \overset{\leftrightarrow}{\partial_\mu} K^-\right), \quad (A.8)$$

$$\mathcal{L}_{\gamma\gamma\Phi\Phi} = e^2 B^\mu B_\mu(\pi^+\pi^- + K^+K^-)\,, \quad (A.9)$$

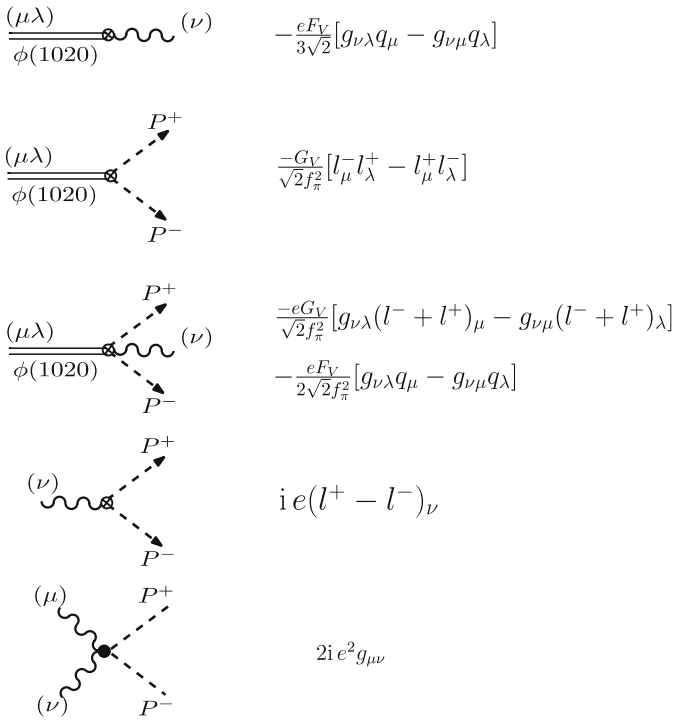

Fig. 6. The $\mathcal{O}(p^2)$ vertices from the chiral Lagrangian L^{A} (A.1). The *dash line* stands for the kaon, the *double solid* line for the vector meson ϕ, the *wavy line* for the photon

where for any a and b the notation $a \overset{\leftrightarrow}{\partial_\mu} b \equiv a\partial_\mu b - b\partial_\mu a$ is introduced. We have

$$\mathcal{L}_{\gamma V} = eF_V F^{\mu\nu}\left(\frac{1}{2}\rho^0_{\mu\nu} + \frac{1}{6}\omega_{\mu\nu} - \frac{1}{3\sqrt{2}}\phi_{\mu\nu}\right), \quad (A.10)$$

$$\begin{aligned}\mathcal{L}_{VPP} = \mathrm{i}\frac{G_V}{f_\pi^2}\,[&\rho^0_{\mu\nu}(2\partial^\mu\pi^+\partial^\nu\pi^- + \partial^\mu K^+\partial^\nu K^-) \\ &+ \omega_{\mu\nu}\left(\partial^\mu K^+\partial^\nu K^-\right) \\ &+ \phi_{\mu\nu}\left(-\sqrt{2}\partial^\mu K^+\partial^\nu K^-\right)\Big]\,, \end{aligned} \quad (A.11)$$

$$\begin{aligned}\mathcal{L}_{\gamma VPP} = &-\frac{eF_V}{f_\pi^2}\partial^\mu B^\nu \rho^0_{\mu\nu}\pi^+\pi^- \\ &- \frac{eF_V}{2f_\pi^2}\partial^\mu B^\nu\left(\rho^0_{\mu\nu} + \omega_{\mu\nu} - \sqrt{2}\phi_{\mu\nu}\right)K^+K^- \\ &- \frac{2eG_V}{f_\pi^2}B^\nu\rho^0_{\mu\nu}\left(\pi^+\partial^\mu\pi^- + \pi^-\partial^\mu\pi^+\right) \\ &- \frac{eG_V}{f_\pi^2}B^\nu\left(\rho^0_{\mu\nu} + \omega_{\mu\nu} - \sqrt{2}\phi_{\mu\nu}\right) \\ &\times\left(K^+\partial^\mu K^- + K^-\partial^\mu K^+\right). \end{aligned} \quad (A.12)$$

From these terms one can derive the $\mathcal{O}(p^2)$ vertex functions shown in Fig. 6.

The chiral couplings F_V and G_V can be extracted from the vector meson partial widths [25, 44]. From (A.10) and (A.11) one calculates the following decay widths:

$$\Gamma_{\rho\to\pi\pi} = \frac{G_V^2}{48\pi f_\pi^4}\left(M_\rho^2 - 4m_\pi^2\right)^{3/2}\,, \quad (A.13)$$

Table 7. Values of the electromagnetic coupling constants for the vector mesons

ρ^0		ω		ϕ	
$\Gamma_{\rho\to e^+e^-}$, keV	F_V (MeV)	$\Gamma_{\omega\to e^+e^-}$, keV	F_V (MeV)	$\Gamma_{\phi\to e^+e^-}$, keV	F_V (MeV)
7.02 ± 0.11	156.162	0.60 ± 0.02	137.629	1.27 ± 0.04	161.629
$\Gamma_{\rho\to\mu^+\mu^-}$, keV	F_V (MeV)	$\Gamma_{\omega\to\mu^+\mu^-}$, keV	F_V (MeV)	$\Gamma_{\phi\to\mu^+\mu^-}$, keV	F_V (MeV)
6.66 ± 0.20	152.358	0.76 ± 0.26	154.98	1.21 ± 0.08	157.738

Table 8. Values of the vector-meson coupling to the two pseudoscalar mesons (all values are in MeV)

		$\pi^+\pi^-$	K^+K^-	$K^0\bar{K}^0$
ρ^0	exp. width:	146.4	–	–
	G_V:	65.183	–	–
	$2\,G_V$:	130.366	–	–
ω	exp. width:	0.144 (suppressed)	–	–
ϕ	exp. width:	–	2.096	1.448
	G_V:	–	53.09	54.45
	$2\,G_V$:	–	106.18	108.9

$$\Gamma_{\rho\to e^+e^-}=\frac{e^4F_V^2}{12\pi M_\rho}\,. \tag{A.14}$$

For the decays $\phi\to KK$, $\omega\to e^+e^-$ and $\phi\to e^+e^-$ one has to take into account the SU(3) relations for the strong and electromagnetic couplings implemented in (A.8)–(A.12). Tables 7 and 8 show the values for G_V and F_V that are obtained from the experimental widths.

The condition $F_V=2G_V$ is important for amplitudes to converge (see Sect. 2.3). From Tables 7 and 8 one sees that this relation is satisfied only approximately, and the closest values are obtained from (A.13) and (A.14) for the decays $\rho\to\pi^+\pi^-$ and $\rho\to e^+e^-$.

Appendix B: Chiral Lagrangian for light scalar mesons

The $\mathcal{O}(p^2)$ ChPT Lagrangian, which explicitly incorporates the scalar mesons and their interactions with the pseudoscalars reads [25]

$$\begin{aligned}L^{\rm B}&=c_d\left\langle S^{\rm oct}u_\mu u^\mu\right\rangle+c_m\left\langle S^{\rm oct}\chi_+\right\rangle\\&\quad+\tilde{c}_dS^{\rm sing}\left\langle u_\mu u^\mu\right\rangle+\tilde{c}_mS^{\rm sing}\left\langle\chi_+\right\rangle\,,\end{aligned} \tag{B.1}$$

and $\chi_+=u^+\chi u^++u\chi u$. For definitions see Appendix A and [25].

The scalar octet $S^{\rm oct}$ and singlet $S^{\rm sing}$ have the a priori independent couplings c_d and c_m, and those with hats $\tilde{c}_d$ and $\tilde{c}_m$. The numerical values of these couplings are determined by the underlying QCD. However, it is difficult to find c_d, c_m, $\tilde{c}_d$ and $\tilde{c}_m$ at energies about 1 GeV because of the non-perturbative regime of QCD. From the assumption of a large number of quark colors ($N_c\to\infty$) it was shown [25] that the octet and singlet (with "tilde") chiral couplings obey the relations

$$\tilde{c}_m=\mu\frac{c_m}{\sqrt{3}}\,,\quad \tilde{c}_d=\mu\frac{c_d}{\sqrt{3}}\,,\quad \mu=\pm1\,. \tag{B.2}$$

The applicability of (B.2) to the scalar meson radiative decays gives rise to some doubts (see [18], for instance). Anyway we use these constraints to reduce the number of independent parameters in Sect. 3.1.

For the description of the scalar meson radiative decays we expand u_μ in (B.1) in a series in Φ. The $\mathcal{O}(p^2)$ interaction with the scalar mesons is defined by

$$\begin{aligned}L^{\rm B}&=L^{\rm ChPT}_{\rm octet}+L^{\rm ChPT}_{\rm singlet}\,,\\L^{\rm ChPT}_{\rm octet}&=\frac{2c_d}{f_\pi^2}\left\langle S^{\rm oct}\partial_\mu\Phi\partial^\mu\Phi\right\rangle\\&\quad-{\rm i}\frac{2ec_d}{f_\pi^2}B^\mu\left\langle S^{\rm oct}\{\partial_\mu\Phi,[Q,\Phi]\}\right\rangle\\&\quad-\frac{2e^2c_d}{f_\pi^2}B^\mu B_\mu\left\langle S^{\rm oct}[Q,\Phi]^2\right\rangle\\&\quad-\frac{c_m}{f_\pi^2}\left\langle S^{\rm oct}\Phi\{\chi,\Phi\}\right\rangle+\frac{2c_m}{f_\pi^2}\left\langle S^{\rm oct}\chi\right\rangle\,,\\L^{\rm ChPT}_{\rm singlet}&=\frac{2\tilde{c}_d}{f_\pi^2}\left\langle\partial_\mu\Phi\partial^\mu\Phi\right\rangle S^{\rm sing}\\&\quad+{\rm i}\frac{4e\tilde{c}_d}{f_\pi^2}B^\mu\left\langle\partial_\mu\Phi,[Q,\Phi]\right\rangle S^{\rm sing}\\&\quad-\frac{2e^2\tilde{c}_d}{f_\pi^2}B^\mu B_\mu\left\langle[Q,\Phi]^2\right\rangle S^{\rm sing}\\&\quad-2\frac{\tilde{c}_m}{f_\pi^2}\left\langle\chi\Phi^2\right\rangle S^{\rm sing}+\frac{2\tilde{c}_m}{f_\pi^2}\left\langle\chi\right\rangle S^{\rm sing}\,.\end{aligned} \tag{B.3}$$

Apparently the Lagrangian (B.3) does not yield a direct contact coupling of the scalar meson to two photons.

In order to apply (B.3) to the physical scalar fields one has to assume a certain multiplet decomposition, (1). This has to be consistent with phenomenology. The prominent feature of a_0 is its dominant decay to $\pi\eta$. KLOE [1] showed almost no contribution of the $f_0(980)$ resonance in comparison with $a_0(980)$ in the reaction $\phi(1020)\to\gamma\pi^0\eta$. Thus we suppose that the isovector $a_0(980)$ and the isoscalar $f_0(980)$ do not mix. Violation of isospin conservation, related to a possible a_0–f_0 mixing, is a subject for a separate work. This issue can be studied for example by means of the $dd\to({}^4{\rm He}a_0^0\to)\,{}^4{\rm He}\pi^0\eta$ reaction at COSY [49].

As far as we are interested in physical scalar fields, which are combinations of singlet and octet states, it is convenient to introduce effective couplings $g_{S\ldots}$ constructed

Table 9. Effective couplings and their chiral powers for the scalar mesons

$$
\begin{aligned}
g_{f\pi\pi} &= -m_\pi^2\left(4\tilde{c}_m\cos\theta - 2\sqrt{2/3}c_m\sin\theta\right),\\
g_{f\eta\eta} &= -(4/3)\tilde{c}_m\left(4m_K^2 - m_\pi^2\right)\cos\theta\\
&\quad -2\sqrt{2}/\left(3\sqrt{3}\right)c_m\left(8m_K^2 - 5m_\pi^2\right)\sin\theta), \qquad \mathcal{O}(p^2)\\
g_{fKK} &= -m_K^2\left(4\tilde{c}_m\cos\theta + \sqrt{2/3}c_m\sin\theta\right).\\
\hat{g}_{f\pi\pi} &= 4\tilde{c}_d\cos\theta - 2\sqrt{2/3}c_d\sin\theta,\\
\hat{g}_{f\eta\eta} &= 4\tilde{c}_d\cos\theta + 2\sqrt{2/3}c_d\sin\theta, \qquad \mathcal{O}(p^0)\\
\hat{g}_{fKK} &= 4\tilde{c}_d\cos\theta + \sqrt{2/3}c_d\sin\theta.\\
g_{\sigma\pi\pi} &= -m_\pi^2\left(4\tilde{c}_m\sin\theta + 2\sqrt{2/3}c_m\cos\theta\right),\\
g_{\sigma\eta\eta} &= -(4/3)\tilde{c}_m\left(4m_K^2 - m_\pi^2\right)\sin\theta\\
&\quad +2\sqrt{2}/\left(3\sqrt{3}\right)c_m\left(8m_K^2 - 5m_\pi^2\right)\cos\theta), \qquad \mathcal{O}(p^2)\\
g_{\sigma KK} &= -m_K^2\left(4\tilde{c}_m\sin\theta - \sqrt{2/3}c_m\cos\theta\right).\\
\hat{g}_{\sigma\pi\pi} &= 4\tilde{c}_d\sin\theta + 2\sqrt{2/3}c_d\cos\theta,\\
\hat{g}_{\sigma\eta\eta} &= 4\tilde{c}_d\sin\theta - 2\sqrt{2/3}c_d\cos\theta, \qquad \mathcal{O}(p^0)\\
\hat{g}_{\sigma KK} &= 4\tilde{c}_d\sin\theta - \sqrt{2/3}c_d\cos\theta.\\
g_{aKK} &= -\sqrt{2}c_m m_K^2, \qquad \mathcal{O}(p^2)\\
g_{a\pi\eta} &= -2\mathcal{Z}\sqrt{2/3}c_m m_\pi^2.\\
\hat{g}_{aKK} &= \sqrt{2}c_d, \qquad \mathcal{O}(p^0)\\
\hat{g}_{a\pi\eta} &= 2\mathcal{Z}\sqrt{2/3}c_d.
\end{aligned}
$$

from the constants c_d, c_m, $\tilde{c}_d$ and $\tilde{c}_m$. This allows one to rewrite the Lagrangian in a simpler form.

Let S stand for any scalar field, a_0,f_0 or σ, and P for a pseudoscalar $\vec{\pi}=\pi^0,\pi^\pm$ or $K^\pm$, K^0 and $\bar{K}^0$. Then the Lagrangian (B.3) can be reduced to

$$
\begin{aligned}
L^{\rm B} = \frac{1}{f_\pi^2}\sum_S S\Big[&\frac{g_{S\pi\pi}}{2}\vec{\pi}^2 + \frac{g_{S\eta\eta}}{2}\eta^2 + g_{S\pi\eta}\pi^0\eta\\
&+ g_{SKK}(K^+K^- + (-1)^{I_S}K^0\bar{K}^0) + (\hat{g}_{S\pi\pi}/2)(\partial_\mu\vec{\pi})^2\\
&+ (\hat{g}_{S\eta\eta}/2)(\partial_\mu\eta)^2 + \hat{g}_{S\pi^0\eta}\partial_\mu\pi^0\partial^\mu\eta\\
&+ \hat{g}_{SKK}(\partial_\mu K^+\partial^\mu K^- + (-1)^{I_S}\partial_\mu K^0\partial^\mu\bar{K}^0)\\
&+ g_{S\gamma\pi\pi}eB_\mu\pi^+\overset{\leftrightarrow}{\partial_\mu}\pi^- + g_{S\gamma KK}eB_\mu K^+\overset{\leftrightarrow}{\partial_\mu}K^-\\
&+ g_{S\gamma\gamma\pi\pi}e^2B_\mu B^\mu\pi^+\pi^- + g_{S\gamma\gamma KK}e^2B_\mu B^\mu K^+K^-\Big],
\end{aligned}
\tag{B.4}
$$

where $I_S=0$ for f_0, σ and $I_S=1$ for a_0. We introduced the effective couplings $g_{S\pi\pi}$, $g_{S\eta\eta}$, etc., listed in Table 9. The couplings that are absent in Table 9 are equal to zero. In addition, for any scalar meson S the following relations for the electromagnetic couplings hold:

$$
\begin{aligned}
g_{S\gamma\pi\pi} &= -\mathrm{i}\hat{g}_{\mathrm{S}\pi\pi},\\
g_{S\gamma KK} &= -\mathrm{i}\hat{g}_{SKK},\\
g_{S\gamma\gamma\pi\pi} &= \hat{g}_{\mathrm{S}\pi\pi},\\
g_{S\gamma\gamma KK} &= \hat{g}_{SKK}.
\end{aligned}
\tag{B.5}
$$

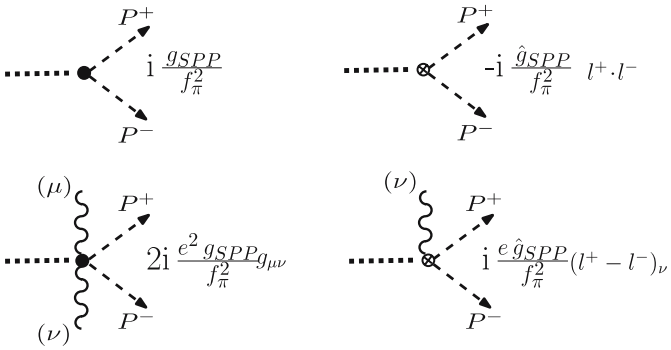

Fig. 7. The $\mathcal{O}(p^2)$ vertices corresponding to the Lagrangian (B.4). The *dotted line* stands for the scalar meson S, the *dashed line* for the pseudoscalar P. Couplings are shown in Table 9; see also (B.5)

Note also that

$$
\mathcal{Z} = \frac{\cos\theta_0 - \sqrt{2}\sin\theta_8}{\cos(\theta_8-\theta_0)} \approx 1.53\,, \tag{B.6}
$$

where the denominator in $\mathcal{Z}$ is equal to the determinant of the transition matrix (A.5) from (η_8,η_0) to (η,η').

The Lagrangian (B.4) leads to the vertices shown in Fig. 7.

Table 9 shows the expressions for the effective couplings as well as the corresponding chiral powers. Some of the couplings include the masses of the Goldstone bosons and are $\mathcal{O}(p^2)$, while the other ones are $\mathcal{O}(p^0)$. Of course, each term in the Lagrangian (B.4) carries a power $\mathcal{O}(p^2)$.

Let us now make a remark on the relation between the sign of the parameter μ in (B.2) and the scalar-meson mixing angle θ in (1). As long as the present consideration does not involve the σ meson we can drop the relation for σ in (1) and observe a non-trivial property: the change $\mu\to-\mu$ is equivalent[5] to the change $\theta\to\pi-\theta$.

Appendix C: Modifications of the model for virtual photons

The complete set of $\mathcal{O}(p^4)$ diagrams has to incorporate all contributions determined by the $\mathcal{O}(p^4)$ Lagrangians (A.8)–(A.12) and (B.4). The Lagrangian (A.10) generates the electromagnetic form factors (FFs) for pseudoscalar particles inside the loops. These FFs should replace the tree-level $PP\gamma$ vertices marked by arrows in Fig. 1, if the FFs do not increase the chiral power of a diagram, and they are calculated from the $\mathcal{O}(p^4)$ Lagrangian.

Note that the electromagnetic FFs of kaons and pions have been studied in various approaches (let us just mention the considerations for on-mass-shell pions [50, 51] and kaons [44]). The FF calculated from the ChPT Lagrangian includes a direct photon–vector-meson transition, i.e. vector-meson dominance, as well as the ordinary

[5] This equivalence is reflected in Table 4.

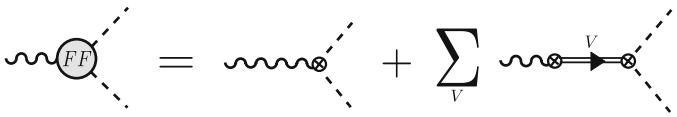

Fig. 8. The $\mathcal{O}(p^2)$ electromagnetic vertex of the (off-mass-shell) pseudoscalar meson in ChPT. All possible intermediate vector resonances $V = \rho^0, \omega, \phi, \ldots$ in general contribute. For real photons only the first term on the r.h.s. is non-zero

contact interaction (see the illustration in Fig. 8 and Appendix A). Fortunately, the real photons do not couple to vector mesons within this approach (see, e.g., [44] for a discussion of this and the one-loop modification of the electromagnetic vertex). Therefore, as long as one is interested in processes with real photons, there are no $\mathcal{O}(p^4)$ diagrams in addition to those shown in Fig. 1, and therefore Fig. 1 gives the complete set of diagrams in this order. A similar reasoning applies to the consideration of the diagrams shown in Fig. 2 and Fig. 3 for $\phi \to \gamma a_0/f_0$ and $f_0/a_0 \to \gamma\rho/\omega$ decay, respectively.

Appendix D: Dimensional regularization. Loop integrals

In the calculation of loop integrals, we use the dimensional regularization method (see, for instance, § 7 and Appendix B in [52]).

The dimension of space-time $D = 4 - 2\epsilon$ in the limit $\epsilon \to 0$ corresponds to that of 4-dimensional Minkowski space. In the text this limit is assumed in all expressions. The integration measure for 4-dimensional space is replaced by that for D-dimensional space: $\mathrm{d}^4 q \to (\Lambda^2)^\epsilon \mathrm{d}^D q$, where the arbitrary regularization parameter Λ has the units of mass. Integrals with this measure are defined via analytical continuation from a space with an integer number of dimensions. The metric tensor obeys the condition $g^{\mu\nu} g_{\mu\nu} = D$. The Dirac matrices satisfy the anti-commutation relations $\{\gamma^\mu, \gamma^\nu\} = 2g^{\mu\nu}$. Here $\gamma^\mu \gamma_\mu = D$, and the ordinary trace formulae are generalized to $\mathrm{Tr}(\gamma^\mu \gamma^\nu) = 2^{D/2} g^{\mu\nu}$, etc.

In a calculation of the loop diagrams the typical integrals presented in Table 10 arise. For divergent terms we define

$$I_\epsilon = 1/\epsilon - \gamma_\epsilon + \ln 4\pi \,.$$

The Euler–Mascheroni constant $\gamma_\epsilon \approx 0.57721566490$ can be expressed in terms of the gamma-function derivative: $\gamma_\epsilon = -\Gamma'(1) = -\int_0^\infty \mathrm{d}x \exp(-x) \ln x$.

Table 10. Table of typical D-dimensional integrals (for any vector Q^μ and complex number R)

$$\begin{aligned}
\Lambda^{2\epsilon} \textstyle\int \frac{\mathrm{d}^D l}{(2\pi)^D} \frac{1}{l^2 + R} &= \frac{-\mathrm{i}R}{(4\pi)^2} \left[I_\epsilon + 1 - \ln\left(\frac{-R}{\Lambda^2}\right) \right], \\
\Lambda^{2\epsilon} \textstyle\int \frac{\mathrm{d}^D l}{(2\pi)^D} \frac{\{1, l^\mu l^\nu\}}{(l^2 - 2l\cdot Q + R)^2} &= \{1, Q^\mu Q^\nu\} \frac{\mathrm{i}}{(4\pi)^2} \\
&\quad \times \left[I_\epsilon - \ln\left(\frac{Q^2 - R}{\Lambda^2}\right) \right] \\
&\quad + \{0, g^{\mu\nu}\} \frac{\mathrm{i}}{32\pi^2} (Q^2 - R) \\
&\quad \times \left[I_\epsilon + 1 - \ln\left(\frac{Q^2 - R}{\Lambda^2}\right) \right], \\
\Lambda^{2\epsilon} \textstyle\int \frac{\mathrm{d}^D l}{(2\pi)^D} \frac{\{1, l^\alpha, l^\alpha l^\beta, l^\alpha l^\beta l^\nu\}}{(l^2 - 2l\cdot Q + R)^3} &= \frac{-\mathrm{i}}{2(4\pi)^2} \frac{\{1, Q^\alpha, Q^\alpha Q^\beta, Q^\alpha Q^\beta Q^\nu\}}{Q^2 - R} \\
&\quad + \frac{\mathrm{i}}{4(4\pi)^2} \left[I_\epsilon - \ln\left(\frac{Q^2 - R}{\Lambda^2}\right) \right] \\
&\quad \times \{0, 0, g^{\alpha\beta}, (g^{\alpha\beta} Q^\nu \\
&\quad + g^{\alpha\nu} Q^\beta + g^{\nu\beta} Q^\alpha)\},
\end{aligned}$$

References

1. KLOE Collaboration, A. Aloisio et al., Phys. Lett. B **536**, 209 (2002) [arXiv:hep-ex/0204012]
2. KLOE Collaboration, A. Aloisio et al., Phys. Lett. B **537**, 21 (2002) [arXiv:hep-ex/0204013]
3. SND Collaboration, M.N. Achasov et al., Phys. Lett. B **479**, 53 (2000)
4. CMD-2 Collaboration, R.R. Akhmetshin et al., Phys. Lett. B **462**, 380 (1999)
5. N.N. Achasov, V.N. Ivanchenko, Nucl. Phys. B **315**, 465 (1989)
6. D. Black, M. Harada, J. Schechter, Phys. Rev. D **73**, 054 017 (2006)
7. BES Collaboration, M. Ablikim et al., Phys. Lett. B **607**, 243 (2005) [arXiv:hep-ex/0411001]
8. D.V. Bugg, Phys. Rep. **397**, 257 (2004) [arXiv:hep-ex/0412045]
9. M.R. Pennington, arXiv:hep-ph/0309228
10. M.R. Pennington, Int. J. Mod. Phys. A **21**, 747 (2006) [arXiv:hep-ph/0509265]
11. J.D. Weinstein, N. Isgur, Phys. Rev. D **41**, 2236 (1990)
12. R.H. Lemmer, Phys. Lett. B **650**, 152 (2007) [arXiv:hep-ph/0701027]
13. Y.S. Kalashnikova, A.E. Kudryavtsev, A.V. Nefediev, C. Hanhart, J. Haidenbauer, Eur. Phys. J. A **24**, 437 (2005) [arXiv:hep-ph/0412340]
14. C. Hanhart, Y.S. Kalashnikova, A.E. Kudryavtsev, A.V. Nefediev, Phys. Rev. D **75**, 074 015 (2007) [arXiv:hep-ph/0701214]
15. J.A. Oller, E. Oset, A. Ramos, Prog. Part. Nucl. Phys. **45**, 157 (2000) [arXiv:hep-ph/0002193]
16. A. Dobado, J.R. Pelaez, Phys. Rev. D **56**, 3057 (1997) [arXiv:hep-ph/9604416]
17. R.L. Jaffe, arXiv:hep-ph/0701038
18. J.R. Pelaez, Phys. Rev. Lett. **92**, 102 001 (2004) [arXiv:hep-ph/0309292]
19. Y. Kalashnikova, A. Kudryavtsev et al., Phys. Rev. C **73**, 045 203 (2006)
20. H.-H. Adam, M. Bashkanov et al. arXiv:nucl-ex/0411038
21. F. Ambrosino et al., Eur. Phys. J. C **50**, 729 (2007) [arXiv:hep-ex/0603056]
22. F. Close, N. Isgur, S. Kumano, Nucl. Phys. B **389**, 513 (1993)
23. J. Vijande, A. Valcarce, F. Fernandez, B. Silvestre-Brac, Phys. Rev. D **72**, 034 025 (2005) [arXiv:hep-ph/0508142]
24. D. Black, M. Harada, J. Schechter, Phys. Rev. Lett. **88**, 181 603 (2002) [arXiv:hep-ph/0202069v2]
25. G. Ecker, J. Gasser, A. Pich, E. de Rafael, Nucl. Phys. B **321**, 311 (1989)

26. E. Klempt, Acta Phys. Pol. B **29**, 3367 (1998)
27. G. Ecker, Prog. Part. Nucl. Phys. **35**, 1 (1995) [arXiv:hep-ph/9501357]
28. M. Bando, T. Kugo, K. Yamawaki, Phys. Rep. **164**, 217 (1988)
29. Ulf G. Meißner, Phys. Rep. **161**, 213 (1988)
30. G. Ecker, J. Gasser, H. Leutwyler, A. Pich, Phys. Lett. B **223**, 425 (1989)
31. Belle Collaboration, T. Mori et al., Phys. Rev. D **75**, 051 101 (2007) [arXiv:hep-ex/0610038]
32. Particle Data Group, W.-M. Yao et al., J. Phys. G: Nucl. Part. Phys. **33**, 1 (2006)
(URL: http://pdg.lbl.gov)
33. CLEO Collaboration, H. Muramatsu et al., Phys. Rev. Lett. **89**, 21 802 (2002)
34. CLEO Collaboration, H. Muramatsu et al., Phys. Rev. Lett. **90**, 059 901 (2002) [Erratum]
35. L. Maiani, F. Piccinini, A.D. Polosa, V. Riquer, Phys. Rev. Lett. **93**, 212 002 (2004) [arXiv:hep-ph/0407017]
36. S. Fajfer, Phys. Rev. D **51**, 1101 (1995) [arXiv:hep-ph/9406377]
37. N.N. Achasov, A.V. Kiselev, Phys. Rev. D **70**, 111 901 (2004) [arXiv:hep-ph/0405128]
38. J.A. Oller, Nucl. Phys. A **714**, 161 (2003) [arXiv:hep-ph/0205121]
39. J.A. Oller, Nucl. Phys. A **727**, 353 (2003) [arXiv:hep-ph/0306031]
40. E. Klempt, B.C. Metsch, C.R. Muenz, H.R. Petry, Phys. Lett. B **361**, 160 (1995)
41. KLOE Collaboration, F. Ambrosino et al., Phys. Lett. B **634**, 148 (2006) [arXiv:hep-ex/0511031]
42. P. Franzini, In: Proc. of Workshop on e^+e^- in the 1-GeV to 2-GeV Range: Physics and Accelerator Prospects – ICFA Mini-workshop – Working Group on High Luminosity e^+e^- Colliders, Alghero, Sardinia, Italy, 10–13 Sep 2003, pp. SAPL003, arXiv:hep-ex/0401031
43. F. Ambrosino et al., Eur. Phys. J. C **50**, 729 (2007) [arXiv:hep-ex/0603056]
44. S.A. Ivashyn, A.Y. Korchin, Eur. Phys. J. C **49**, 697 (2007) [arXiv: hep-ph/0611039]
45. J. Prades, Z. Phys. C **63**, 491 (1994)
46. J. Prades, Eur. Phys. J. C **11**, 571 (1999) [Erratum]
47. N. Beisert, B. Borasoy, arXiv:hep-ph/0107175
48. T. Feldmann, P. Kroll, B. Sted, Phys. Rev. D **58**, 114 006 (1998) [arXiv:hep-ph/9802409]
49. C. Hanhart, AIP Conf. Proc. **688**, 61 (2004) [arXiv: nucl-th/0306073]
50. S.K. Dubinsky, A.Y. Korchin, N.P. Merenkov, Zh. Eksp. Teor. Fiz. **126**, 259 (2004) [arXiv:hep-ph/0407191]
51. S. Dubinsky, A. Korchin, N. Merenkov, G. Pancheri, O. Shekhovtsova, Eur. Phys. J. C **40**, 41 (2005) [arXiv: hep-ph/0411113]
52. F.J. Yndurain, Quantum Chromodynamics (Springer, New York Berlin Heidelberg Tokyo, 1983)